

**Project Report  
ATC-154**

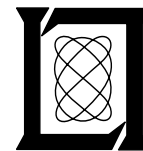
# **A Comparison of PAM-II and FLOWS Mesonet Data During COHMEX**

**M.M. Wolfson  
M.J. Iacono**

23 December 1987

---

**Lincoln Laboratory**  
MASSACHUSETTS INSTITUTE OF TECHNOLOGY  
*LEXINGTON, MASSACHUSETTS*



Prepared for the Federal Aviation Administration,  
Washington, D.C. 20591

This document is available to the public through  
the National Technical Information Service,  
Springfield, VA 22161

This document is disseminated under the sponsorship of the Department of Transportation in the interest of information exchange. The United States Government assumes no liability for its contents or use thereof.

TECHNICAL REPORT STANDARD TITLE PAGE

1. Report No. DOT/FAA/PM-87/36	2. Government Accession No.	3. Recipient's Catalog No.	
4. Title and Subtitle A Comparison of PAM-II and FLOWS Mesonet Data During COHMEX		5. Report Date 23 December 1987	
		6. Performing Organization Code	
7. Author(s) Marilyn M. Wolfson and Michael J. Iacono		8. Performing Organization Report No. ATC-154	
9. Performing Organization Name and Address Lincoln Laboratory, MIT P.O. Box 73 Lexington, MA 02173-0073		10. Work Unit No. (TRAVIS)	
		11. Contract or Grant No. DTFA-01-80-Y-10546	
		13. Type of Report and Period Covered Project Report	
12. Sponsoring Agency Name and Address Department of Transportation Federal Aviation Administration Program Engineering Service Washington, DC 20591		14. Sponsoring Agency Code	
15. Supplementary Notes  The work reported in this document was performed at Lincoln Laboratory, a center for research operated by Massachusetts Institute of Technology, under Air Force Contract F19628-85-C-0002.			
16. Abstract  Surface weather stations are being used in the Terminal Doppler Weather Radar program to assess the radar detectability of wind shear and to help gain an understanding of microburst forcing mechanisms. During 1986, surface station networks operated by Lincoln Laboratory (FLOWS) and the National Center for Atmospheric Research (PAM-II) were deployed in the Huntsville, AL area. A preliminary assessment of the overall performance of PAM-II and FLOWS networks suggests that they performed with comparable accuracy for those meteorological characteristics most important to the detection of microbursts. While differences and discrepancies were noted, especially in the network total precipitation amounts, none would preclude treating PAM-II and FLOWS data together as if they were generated by a single network. We conclude that the data can be directly combined for microburst detection analyses.			
17. Key Words PAM-II FLOWS meteorological instrumentation automatic weather station  downburst microburst thunderstorms COHMEX MIST mesonet wind shear		18. Distribution Statement  Document is available to the public through the National Technical Information Service, Springfield, VA 22161.	
19. Security Classif. (of this report) Unclassified	20. Security Classif. (of this page) Unclassified	21. No. of Pages 58	22. Price

## CONTENTS

Abstract	ii
Acknowledgements	iii
List of Acronyms	iv
List of Figures	v
List of Tables	vii
I. INTRODUCTION	1
II. AVERAGING METHODS	7
III. PERFORMANCE	9
IV. PRODUCT DIFFERENCES	11
A. Average and Peak Wind Speed	11
B. Wind Direction	16
C. Temperature and Relative Humidity	21
D. Barometric Pressure	26
E. Total Precipitation Amounts	26
V. DOWNBURST EVENT OF 7 JUNE 1986	33
A. Individual Station Comparison	33
B. Network Comparison	36
VI. CONCLUSIONS	45
VII. RECOMMENDATIONS	46
References	47

## ABSTRACT

Surface weather stations are being used in the Terminal Doppler Weather Radar program to assess the radar detectability of wind shear and to help gain an understanding of microburst forcing mechanisms. During 1986, surface station networks operated by Lincoln Laboratory (FLOWS) and the National Center for Atmospheric Research (PAM-II) were deployed in the Huntsville, AL area. A preliminary assessment of the overall performance of PAM-II and FLOWS networks suggests that they performed with comparable accuracy for those meteorological characteristics most important to the detection of microbursts. While differences and discrepancies were noted, especially in the network total precipitation amounts, none would preclude treating PAM-II and FLOWS data together as if they were generated by a single network. We conclude that the data can be directly combined for microburst detection analyses.

## ACKNOWLEDGEMENTS

The authors thank the co-principal investigators of the MIST experiment, Drs. T. Theodore Fujita and Roger Wakimoto, for allowing us to use the PAM-II mesonet data. Dr. Fujita performed the analyses shown in Figures 11 and 12 and also supplied the figures themselves. Charles Wade at NCAR provided useful data resulting from his comparison of the PROBE weather stations (from which the FLOWS stations are descended) and the PAM-I system collocated during CCOPE (in Montana in 1981). The inspiration to examine some of the variables presented here came directly from his work. Efforts by John DiStefano and Barbara Forman of Lincoln Laboratory in organizing mesonet data processing and writing the software are gratefully acknowledged. Charles Curtiss was primarily responsible for keeping the FLOWS mesonet operating and his extraordinary efforts are also gratefully acknowledged.

## LIST OF ACRONYMS

CCOPE	Cooperative Convective Precipitation Experiment
COHMEX	Cooperative Huntsville Meteorological Experiment
FAA	Federal Aviation Administration
FLAWS	FAA-Lincoln Laboratory Operational Weather Studies
GOES	Geostationary Operational Environmental Satellite
GMT	Greenwich Mean Time
MIST	Microburst and Severe Thunderstorm Project
NCAR	National Center for Atmospheric Research
PAM	Portable Automated Mesonet
PROBE	Portable Remote Observations of the Environment

## LIST OF FIGURES

Figure No.		Page No.
1	Map showing locations of MIST and FLOWS networks during COHMEX.	3
2	Photograph of a remote PAM-II station. Taken from Brock, <i>et al.</i> (1986).	4
3	Photograph of a FLOWS mesonet station.	5
4	Percentage of missing data during COHMEX for FLOWS and MIST networks.	10
5	Average wind speed comparison data for FLOWS and MIST networks.	12
6	Peak wind speed comparison data for FLOWS and MIST networks.	13
7	Network average wind speed difference vs. MIST average wind speed.	14
8	Plot of the difference between anemometer measured wind speed and tunnel measured wind speed ("DISCREPANCY") vs. the tunnel measured speeds.	15
9	Wind direction comparison data for FLOWS and MIST networks.	17
10	Difference between FLOWS and MIST network average wind direction vs. time of day (GMT) for a high wind speed day and a low wind speed day.	18
11	Azimuthal frequency of 0.0 – 0.5 m/s winds normalized per station per month for all 41 PAM stations during COHMEX (Fujita, 1987).	19
12	Azimuthal frequency of 1.0 – 1.5 m/s winds normalized per station per month for all 30 FLOWS stations during COHMEX (Fujita, 1987).	20
13	Temperature comparison data for FLOWS and MIST networks.	22
14	Relative humidity comparison data for FLOWS and MIST networks.	23
15	Difference between FLOWS and MIST network average temperature vs. time of day (GMT) for a high wind speed day and a low wind speed day.	24



<b>Figure No.</b>		<b>Page No.</b>
16	Network temperature difference vs. MIST average wind speed.	25
17	Pressure comparison data for FLOWS and MIST networks.	27
18	Location of mesonet pairs used for the comparison of network total precipitation amounts.	29
19	Comparison of 24-hour time series plots of data on 7 June 1986	34
20	Surface wind field and temperature contours (every 2 deg. C) over FLOWS and MIST networks on 7 June 1986.	37
21	Total precipitation amounts (mm) for 7 June 1986, 1650–1750 GMT.	39
22	Time series of a) rain rate data and b) peak wind speed data for FLOWS Station No. 15 and MIST Station No. 37 on 7 June 1986.	43
23	Time series of a) rain rate data and b) peak wind speed data during high wind speed event in which FLOWS rainfall measurements may have been suppressed.	44

## LIST OF TABLES

Table No.		Page No.
1	Pairs of stations used for the comparison of total precipitation amounts between the FLOWS and MIST networks.	28
2	Ratio of MIST total rainfall to FLOWS total rainfall for the COHMEX precipitation events listed.	30

## I. INTRODUCTION

The continuous expansion of the air traffic system makes it increasingly necessary to eliminate avoidable threats to aircraft such as hazardous weather. We are here primarily concerned with the turbulent conditions that predominate in and around thunderstorms. The accelerating and rapidly shifting winds near a column of descending air known as a downburst or microburst can reduce an aircraft's lift faster than a pilot can restore it. There is an urgent need to detect such weather conditions and disseminate the information in time to warn pilots and air traffic controllers.

Doppler weather radars are actively being developed which will provide such warnings. The Terminal Doppler Weather Radar (TDWR) program sponsored by the Federal Aviation Administration (FAA) will provide Doppler radars to continuously scan the airspace over major US airports. The FAA has funded Lincoln Laboratory to develop a pulse Doppler weather radar (called FL-2) to be used to detect weather events hazardous to aviation, and to demonstrate the feasibility of the TDWR (Evans and Johnson, 1984).

Surface weather station data describing wind, temperature, relative humidity, pressure, and rainfall are essential to the evaluation of the TDWR system and to the extension of its capabilities. The data collected by automatic weather stations are being used as the principal inputs to assess the ability of pulse Doppler radar to detect and observe wind shear events (DiStefano, 1987). In particular, surface weather station data are used to determine whether wind shear events have gone undetected due to low reflectivity (*i.e.*, inadequate signal-to-noise ratio), beam blockage of the wind shear region, or unfavorable viewing geometries. Surface thermodynamic and rainfall data furnished by automatic weather stations are also critical for understanding wind shear generation mechanisms. Accordingly, a network of 30 automatic weather stations is also being operated by Lincoln Laboratory to provide additional data on the weather events seen by the FL-2 radar.

Budgetary constraints have limited the FAA-Lincoln Laboratory surface data network to 30 stations. A network of approximately 200 stations would be required to verify microburst detection over the 30 km nominal range of the TDWR (*i.e.*, a 2 km average spacing between weather stations). The Cooperative Huntsville Meteorological Experiment (COHMEX), which took place in June and July of 1986, provided an opportunity to collect a large amount of data on microbursts in the humid southeast part of the country by pooling resources with scientists who were also interested in the phenomena.

During COHMEX, two networks of weather stations covering a 400 square mile area near Huntsville, Alabama (see Fig. 1) were operated simultaneously. The National Center for Atmospheric Research (NCAR), which provided facilities for the Microburst and Severe Thunderstorm (MIST) portion of COHMEX, operated 41 of their own portable automated mesonet (PAM-II) stations. An individual PAM-II station is shown in Fig. 2. The FAA-Lincoln Laboratory Operational Weather Studies (FLOWS) portion of COHMEX included the operation of the 30 FAA mesonet stations, one of which is shown in Fig. 3. By collocating the two networks, it was possible to maintain close station spacing and to provide coverage over roughly twice the area as would have been possible with only one network, thus roughly doubling the number of microburst events which could be analyzed.

However, before using the combined surface network data for TDWR performance assessment and algorithm refinement, we must first determine whether the measurements reported by the PAM-II stations and those reported by the FLOWS stations are consistent for the weather events of concern. The primary purpose of this report is to determine whether the data from the two networks were sufficiently comparable to allow their combined or interchangeable use in the analysis of severe weather events.

Each type of station is solar powered and includes a data collection computer and GOES satellite transmitter, wind sensors, a barometer, temperature and humidity sensors, and a rain gage (the data generated by the station and transmitted to the GOES satellite are then downlinked from the satellite and archived at a ground receiving station).

However, there are several notable differences between the stations. FLOWS employs a cup anemometer and wind vane situated 7.5 m above the ground to sense wind speed and direction. Wind speed and direction must be derived for the MIST\* stations because they are equipped with a pair of perpendicular, horizontal, propellor anemometers 10 m above the ground which measure the east and north components of wind velocity. In addition, the FLOWS temperature and relative humidity sensors are housed within a vane aspirator, a long tube which turns into the wind to keep the sensors ventilated. MIST uses fan ventilated dry and wet bulbs to measure temperature and provide the necessary information to derive relative humidity. Finally, precipitation is measured by the FLOWS stations with weighing gages, devices which keep an accumulated total of the water held within their inner buckets (rainfall must be determined from the positive changes in that total). MIST platforms use tipping-bucket rain gages which tip each time they fill to a certain level and add that amount to the

---

\*The NCAR PAM-II stations will be equivalently referred to as either the "MIST" stations or the "PAM" stations throughout this report.

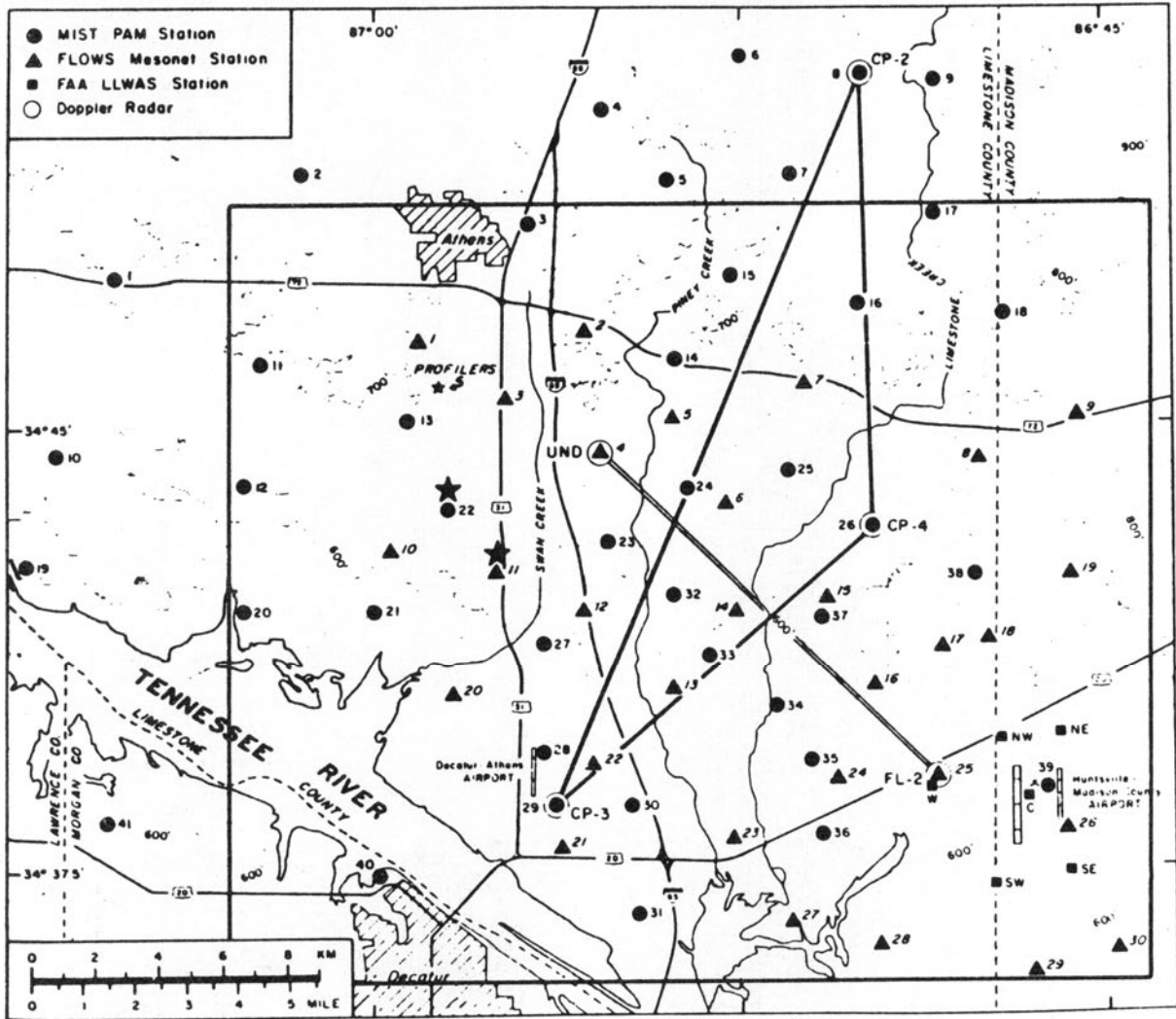


Figure 1. Map showing locations of MIST and FLOWS networks during COHMEX.

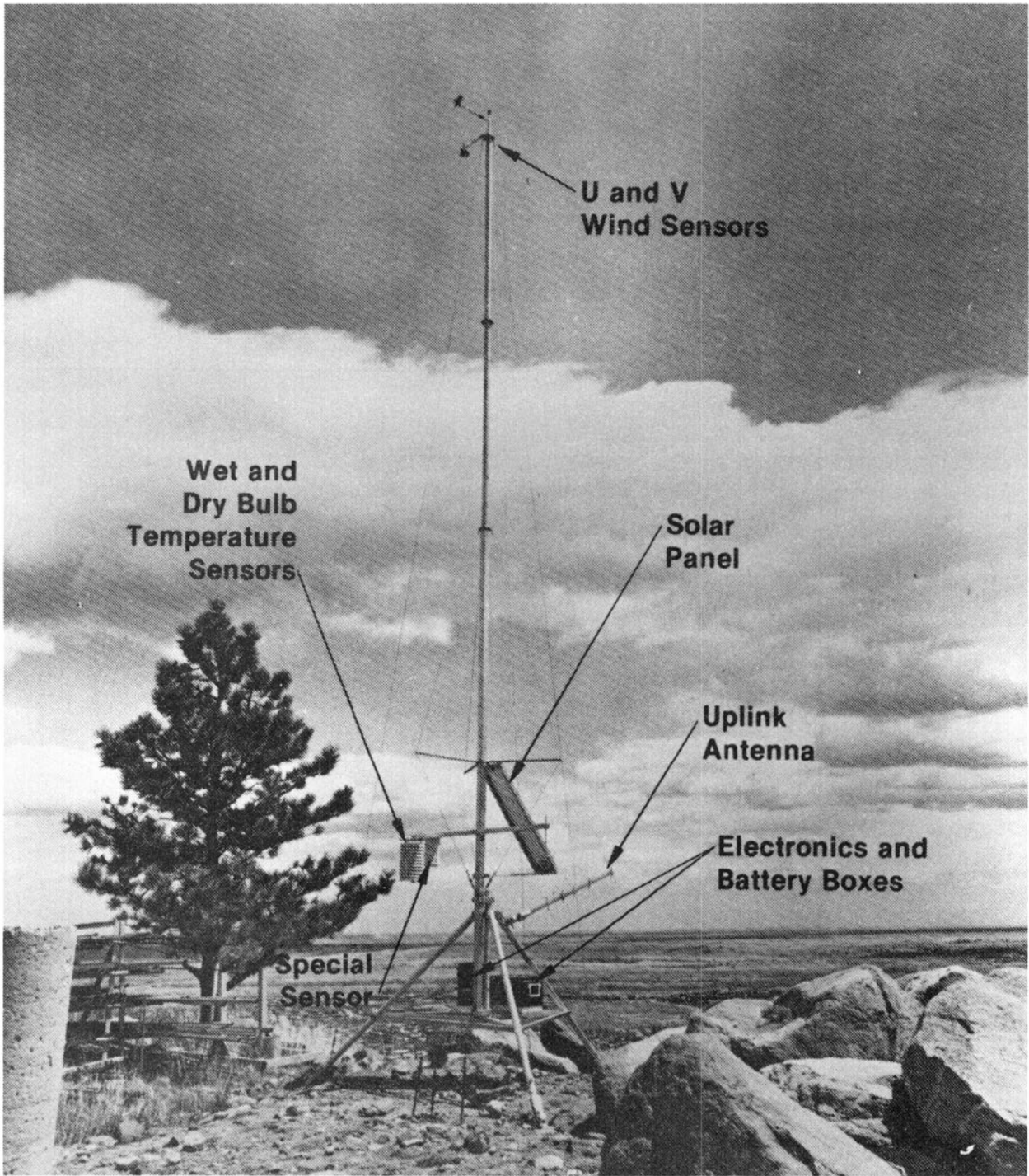


Figure 2. Photograph of a remote PAM-II station. Taken from Brock, et al., (1986).

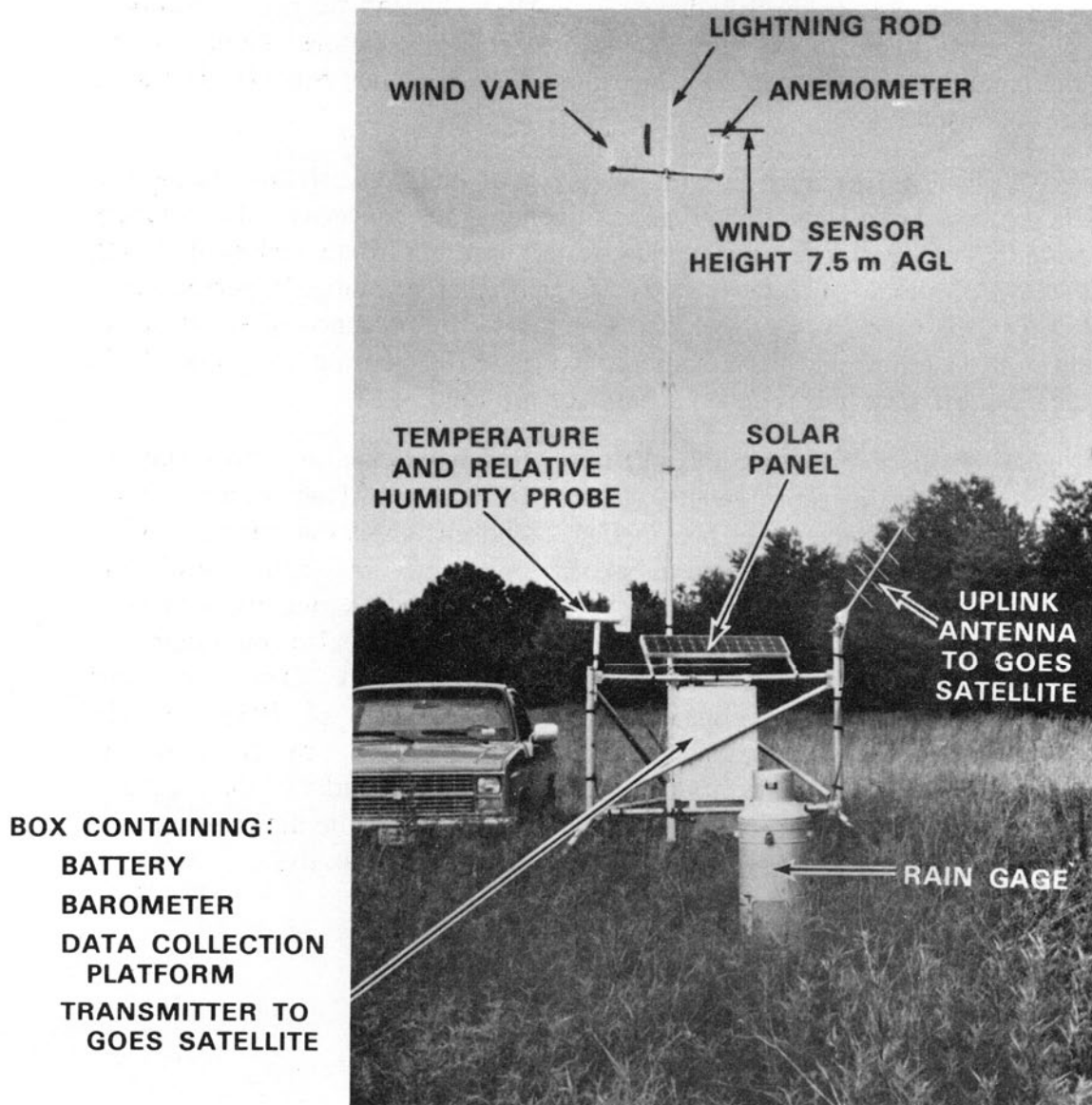


Figure 3. Photograph of a FLOWS mesonet station.



accumulated total. PAM stations are described in detail in Brock and Govind (1977; PAM-I) and Brock *et al.* (1986, PAM-II); FLOWS stations, in Wolfson (1987) and Wolfson *et al.* (1987).

The best way to compare meteorological instruments is to evaluate them together at a site calibrating them to an external control of known accuracy. We were not able to do that during COHMEX. Instead we had to compare each network of instruments to the other as a whole. None of the instruments were co-sited with instruments of the other network, nor were controls used.

This study examines only the accuracy of one network with respect to the other and can come only to general conclusions concerning the accuracy of individual stations. An expanded analysis of the data collected during COHMEX should include a study of each weather station's performance because the networks are intended to indicate the presence of small-scale, short-lived atmospheric phenomena. To do that, accurate and dependable data reported by only a few stations are required.

In order to compare the FLOWS and MIST networks, only those stations which overlap the same general area were included. That area is shown enclosed by the inner bold box in Fig. 1 and encompasses a total of sixty mesonet stations. MIST station No. 22 produced very little useful data during the two month operational period of COHMEX and its data were excluded. A healthy FLOWS station (No. 11) was also eliminated to equalize the number of stations in each network. The remaining twenty-nine FLOWS stations had a mean elevation of 193.6 m. The twenty-nine MIST stations had a mean elevation of 193.8 m. The closeness of these values is important since most of the measured variables used in this study are dependent on elevation, and because it is the network mean of these variables which is the basis of this comparative analysis.



## II. AVERAGING METHODS

The simplest way of comparing the collective data from two networks of mesonet stations is through averaging. Daily averages for each measured variable were computed for all platforms and then for both networks. Although the stations are designed to record weather data in the form of one-minute averages, every minute of data was not necessary to obtain an accurate mean. Therefore, the daily means were determined by averaging four five-minute intervals for each hour and ninety-six for every day (these include days 152-210, or 1 June to 29 July, 1986). The intervals used correspond to minutes 0 to 4, 15 to 19, 30 to 34, and 45 to 49 of each hour. Once calculated for every station, daily network averages for FLOWS and MIST networks can be found for temperature, relative humidity, barometric pressure, average and peak wind speed, and wind direction. Precipitation data were not averaged in this way because they are not absolute measurements of rainfall and thus must be handled differently. (See Section IV E).

A daily mean was not calculated for any platform that had missed more than 10% of its maximum possible data, and that platform was excluded from the network mean calculations for that day. If an entire network was missing more than 15% of its data, then no mean was computed and no comparison was made to the other network for that day. That was done to prevent large data gaps from shifting the mean beyond the point where network comparisons are meaningful.

Standard deviations of the daily means for each station and each network were also computed. The standard deviation of a platform was calculated to reflect its variance from the other twenty-nine stations in the network. This was accomplished with the same 96 five-minute intervals used to find the means. The network mean for each five-minute period was subtracted from the platform's mean at the same interval. This difference was squared, and the squared difference included in a sum across all 96 intervals to provide the variance. All network standard deviations, therefore, were simply averages of the twenty-nine platform deviations.

To show any diurnal influences affecting either network, a second type of average was computed to reveal information on FLOWS and MIST differences as a function of time of day. Using the first five-minutes of each hour, twenty-four averages were performed over all stations and all days. This provided a FLOWS mean and a MIST mean for each variable at each hour of the day.

Finally, note that the averages for the wind products were computed vectorially. This was necessary to remove the problem which arises when values for wind directions that pass through north ( $0^\circ$ ) are

numerically averaged. (For example, a 350° wind and a 10° wind would average numerically to 180° when their true mean is 0°). It also provided a mean resultant wind speed which was typically somewhat lower than a numerical wind speed mean. (For example, a 10 m/s wind from the south and a 10 m/s wind from the west would average numerically to a 10 m/s wind; however the true vector component averages would be 5 m/s each, giving a vector magnitude of 7 m/s). When the wind vectors are averaged, a correct mean wind speed and direction are assured.

### III. PERFORMANCE

Each network's reliability was demonstrated by the consistency with which it transmitted usable data. Every recorded minute of data was included in this part of the analysis. A minute of data was considered bad if it was either missing entirely or suspect. The number of minutes with data missing was totaled for the whole network, averaged over all six variables, and converted to a percentage of the maximum number of minutes for which data were collected. This was plotted for both networks in Fig. 4.

In general, the FLOWS and MIST networks both had less than 10% of their total data missing. Immediately after the worst MIST day (day 188) which had about 10% missing, that network showed improvement which lasted through the last three weeks of COHMEX. FLOWS missing data exceeded 10% on 15 days\* with the worst period occurring during the last week. Most of the missing data on those days were simply not recorded by our commercial down-link service. For the two-month COHMEX period, the MIST network more consistently provided data on a regular basis.

---

\*Day numbers 158, 168, 182, 191, 192, 195, 196, and 205-212.

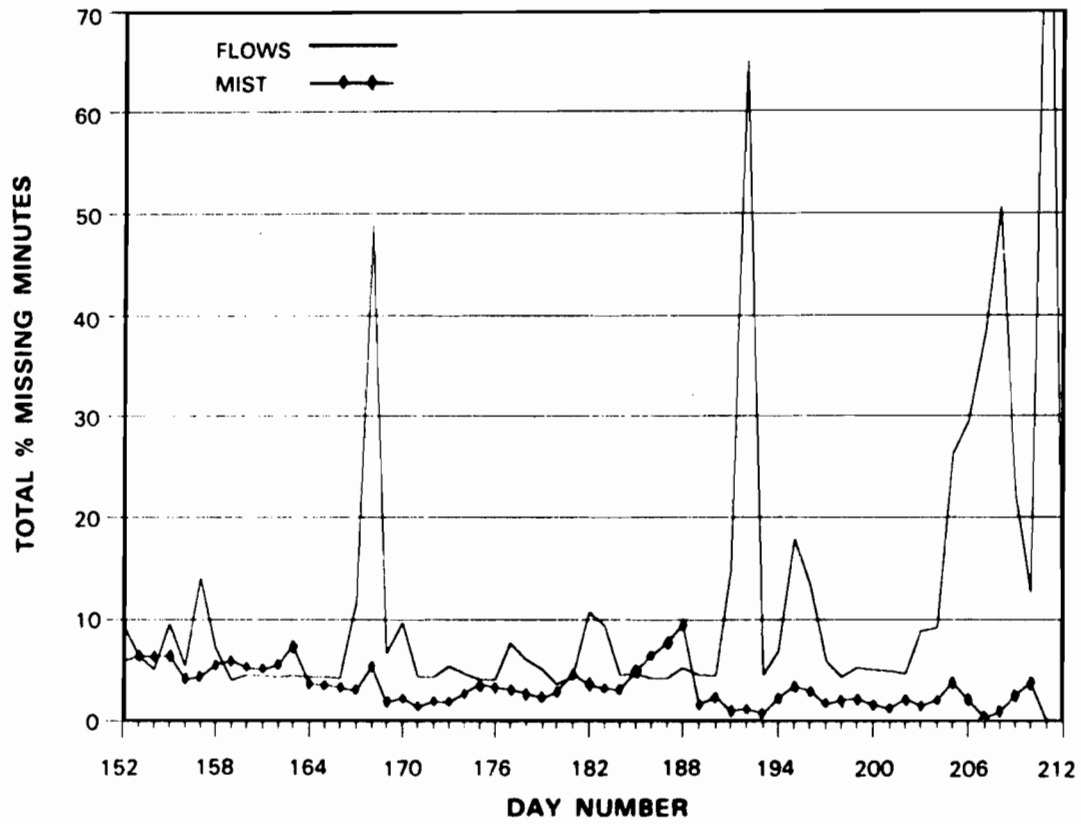


Figure 4. Percentage of missing data during COHMEX for FLOWS and MIST networks.

#### IV. PRODUCT DIFFERENCES

In this section we will discuss the network differences for the following variables: wind speed, wind direction, temperature, relative humidity, barometric pressure, and total precipitation amounts. No differences were calculated on days when the FLOWS network had more than 15% data missing; thus, gaps will be found in plots of network differences and of FLOWS standard deviations as a function of day number.

##### A. Average and Peak Wind Speed

Of all the meteorological variables we examined, wind speed and direction are the most important for the networks to satisfy their purpose of detecting microbursts. Fortunately, FLOWS and MIST achieved their greatest agreement for wind speed and direction, despite the very different methods each uses. Figures 5a and 5b illustrate that agreement for resultant wind speed differences from day to day and for each hour of the day. Figure 5c shows that the standard deviations of wind speed for FLOWS and MIST agree for much of the eight week test period. The results for peak wind speed shown in Fig. 6 similarly agreed.

The most significant discrepancy from the expected results was that FLOWS wind speeds consistently averaged 0.2 m/sec higher than MIST. The FLOWS anemometers were at 7.5 m above ground level and the MIST anemometers, at 10 m. A standard logarithmic wind profile yielded an expected mean MIST wind speed 5% higher than FLOWS as illustrated in Fig. 7. The lower straight line shows the wind speed difference expected theoretically, based on the anemometer height difference. However, for any given MIST wind speed, FLOWS measured a wind speed that was 2–10% greater as shown by the spiked curve in Fig. 7.

Most of the discrepancy between the observed and theoretically predicted wind speed difference could be accounted for by “overspeeding” of the FLOWS anemometers. Wind tunnel experiments show (Fig. 8) that overspeeding of 5.0% to 8.5% always occurs. Since Fig. 8 shows a linear dependence of the wind speed discrepancy on the actual wind speed, it is probable that the manufacturer-specified flow coefficient used in the equation to relate sensor output frequency to wind speed is slightly too large. If 8% is added to the lower boundary in Fig. 7, the result is the upper boundary. Thus, given that overspeeding occurred, FLOWS could be expected to measure slightly higher wind speeds than MIST for the given anemometer heights.

There was another positive discrepancy which could have been due to differences in anemometer calibration, but it amounted to only 3–4%. That could be at least partly attributable to the different methods used to

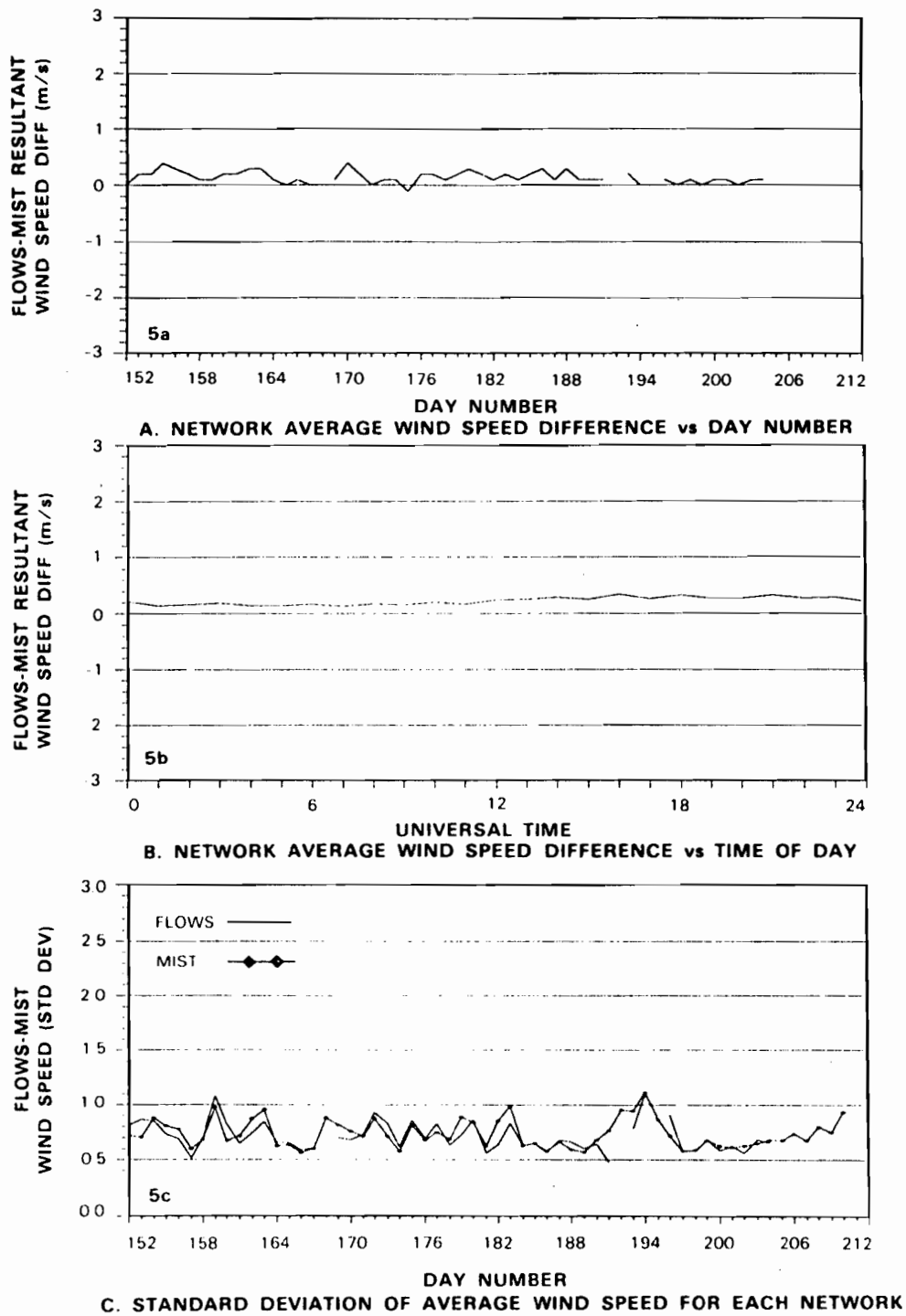


Figure 5. Average wind speed comparison data for FLOWS and MIST networks.

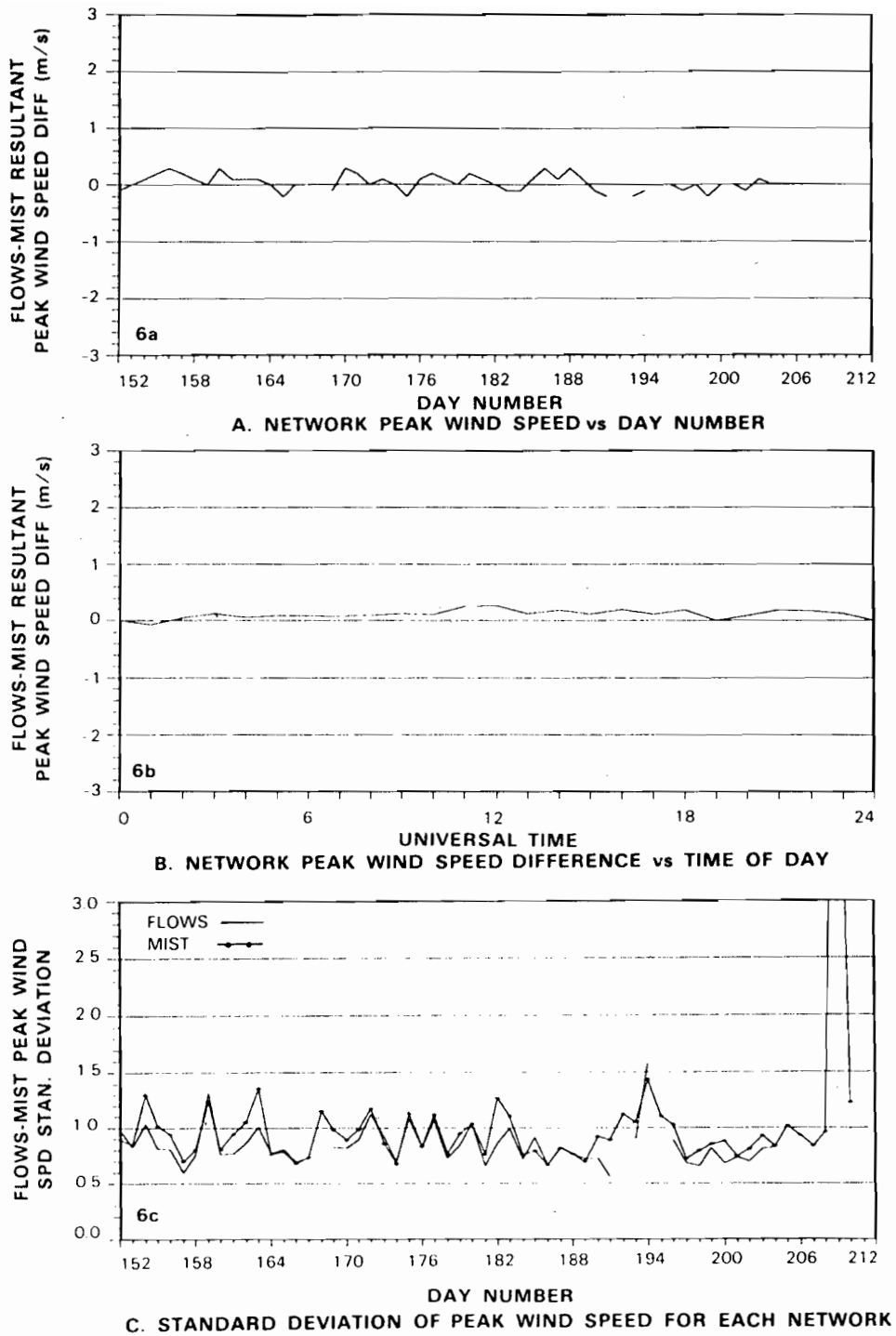


Figure 6. Peak wind speed comparison data for FLOWS and MIST networks.

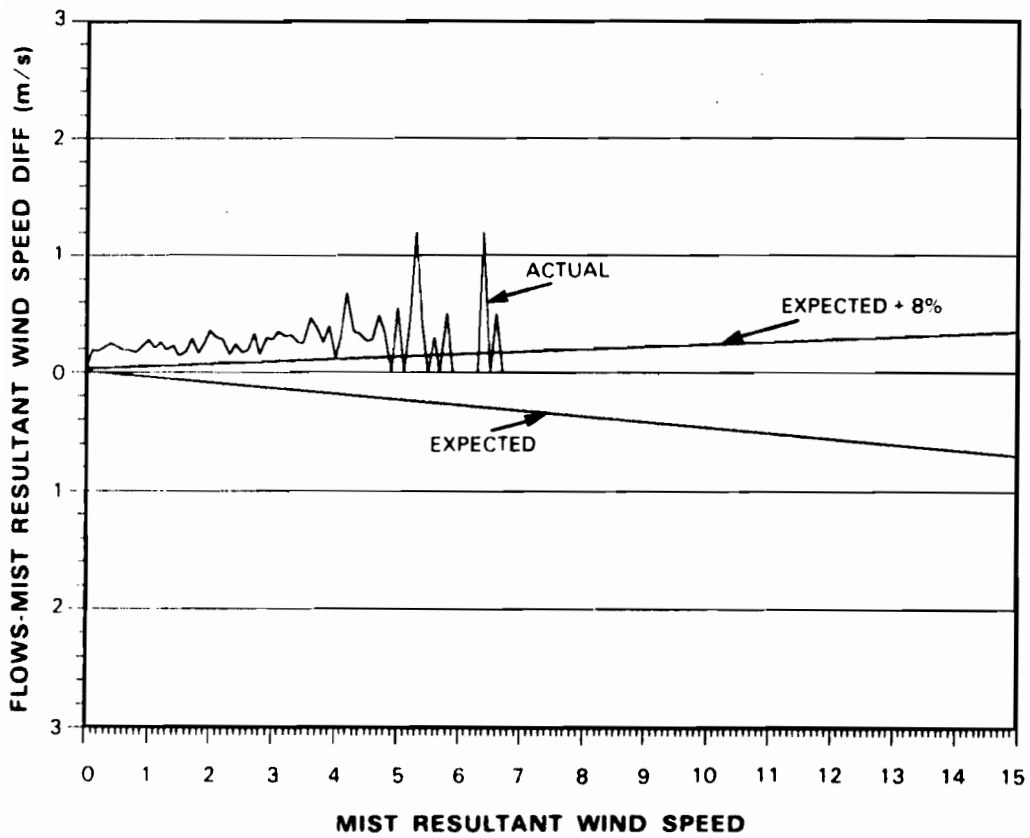


Figure 7. Network average wind speed difference vs. MIST average wind speed.



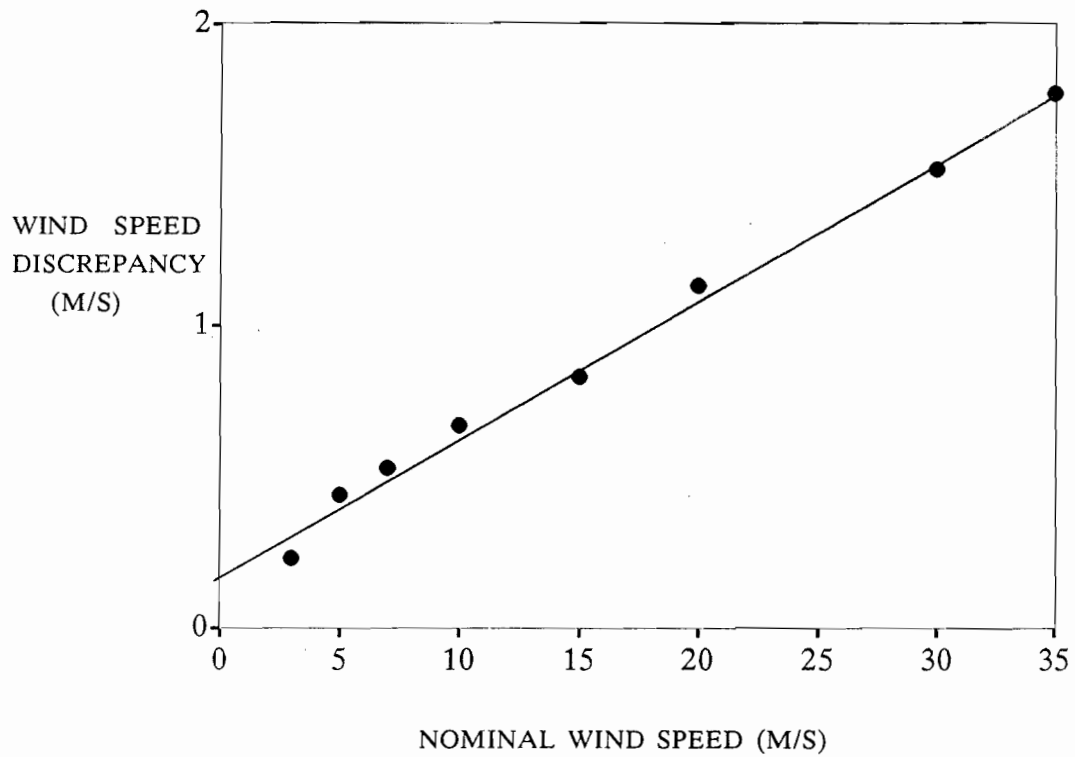


Figure 8. Plot of the difference between anemometer measured wind speed and tunnel measured wind speed (DISCREPANCY) vs. the tunnel measured speeds.

compute the 1-minute average wind speed before transmission of the values to the GOES satellite. In the MIST stations, a true vector average was computed while in the FLOWS stations, the anemometer and wind vane (sine-cosine) outputs were averaged separately. As noted in Chapter II, vector averaging provided a mean resultant wind speed which was somewhat lower than a numerical wind speed mean. (True vector averaging was implemented in the FLOWS stations before their deployment in 1987).

## B. Wind Direction

Wind direction was probably the easiest meteorological parameter to measure accurately once the wind vane was properly oriented. For that reason, FLOWS and MIST showed excellent agreement in their measurements of wind direction. Figure 9 shows the vectorially computed mean wind direction differences for each day and each hour. Figure 9a shows a slight positive tendency of about  $5^\circ$  which indicates that at least a few of the platforms may have been out of alignment. However, since Fig. 9a is a relative comparison of the two networks there is no way to determine from these data whether FLOWS directions were slightly too clockwise or whether MIST directions were slightly too counterclockwise. Magnetic and true north are only  $1^\circ$  apart in the Huntsville area so no compensation was made in the FLOWS data.

Figure 10 demonstrates the drop in the accuracy of wind direction measurements at low wind speed. On 4 June 1986 each network recorded high mean wind speeds and there was near perfect agreement in their measurements of wind direction (Fig. 10a). However, in low wind speed conditions on 1 June 1986 (Fig. 10b) there were large differences in recorded wind direction.

Dr. T. Theodore Fujita, professor of meteorology at the University of Chicago and co-principal investigator of the MIST experiment, has shown that because the MIST wind direction was derived from the east and north speed components, in low winds there would be strongly preferred wind directions (Fig. 11). Preferred wind directions occur at  $0^\circ$  (determined by the absence of a measurable signal from east component),  $90^\circ$  (determined by the absence of a measurable signal from north component),  $45^\circ$  (equal signal from the north and east components),  $63.4^\circ$  (arctangent of 2, or exactly twice the signal from the east component as from the north component), *etc.* The transitions between preferred angles as a function of time would not be smooth. In contrast, the output signals from the sine-cosine potentiometer in the wind vane used to measure wind direction in the FLOWS stations varied smoothly through all angles even in very light wind. Because only the more accurate of the signals (either sine or cosine) was transmitted to the satellite (see, *e.g.*, Wolfson, 1987), there was a small

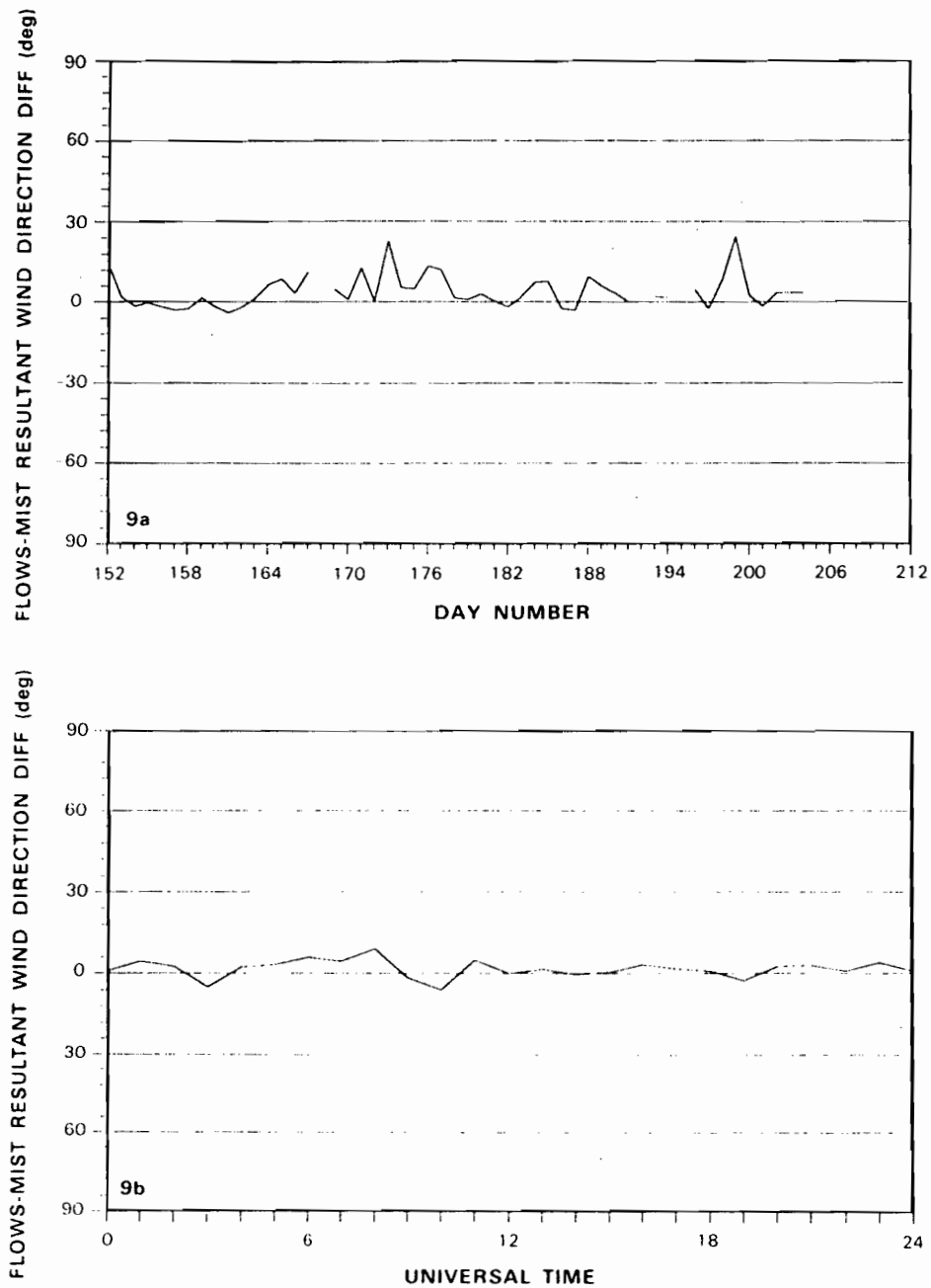
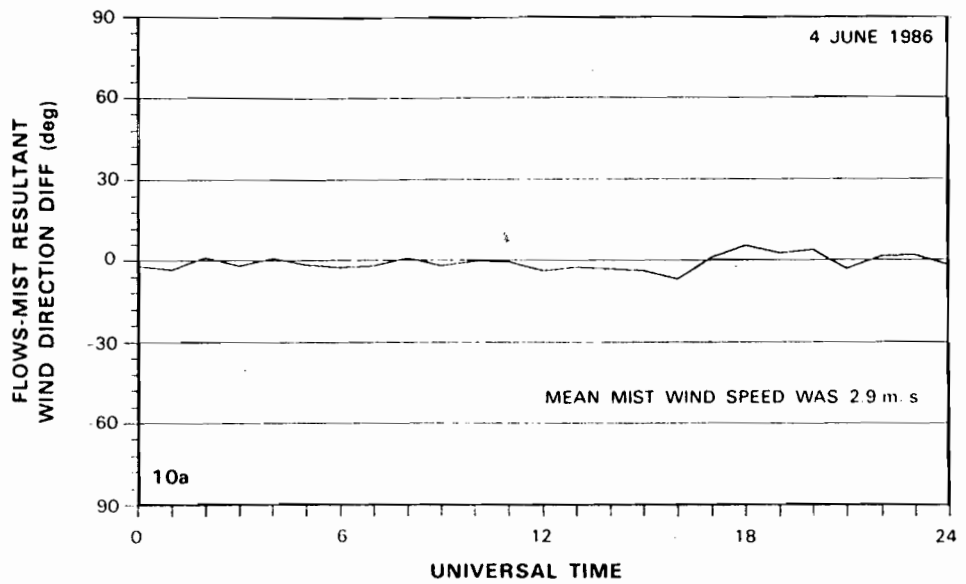
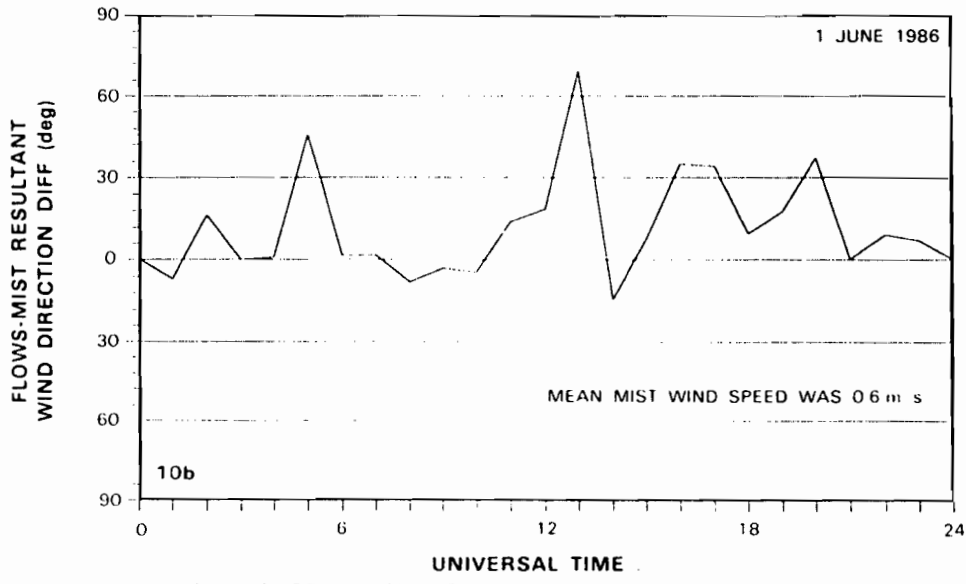


Figure 9. Wind direction comparison data for FLOWS and MIST networks.



A. NETWORK AVERAGE WIND DIRECTION DIFFERENCE vs TIME OF DAY FOR HIGH WIND SPEED DAY



B. NETWORK AVERAGE WIND DIRECTION DIFFERENCE vs TIME OF DAY FOR LOW WIND SPEED DAY

Figure 10. Difference between FLOWS and MIST network average wind direction vs. time of day (GMT) for a high wind speed day and a low wind speed day.

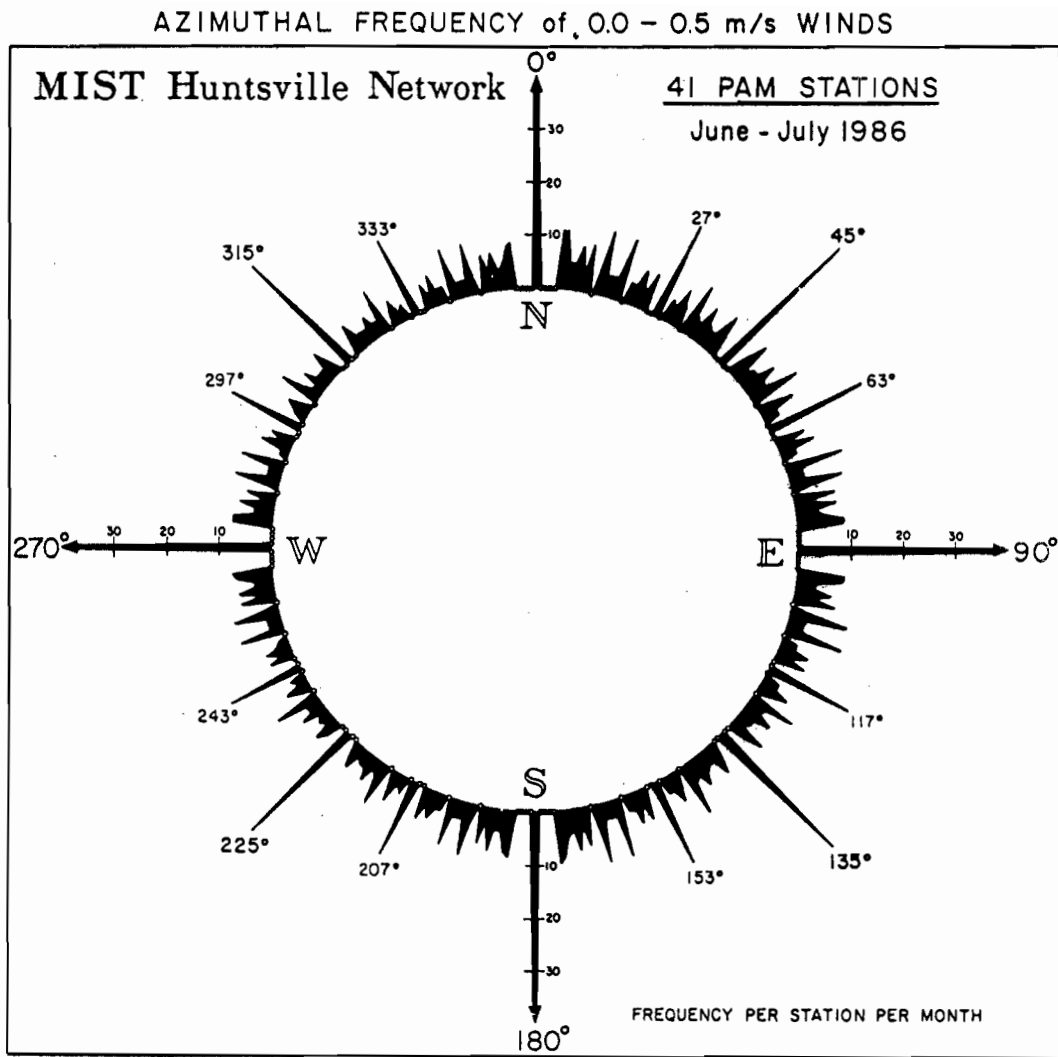


Figure 11. Azimuthal frequency of 0.0 - 0.5 m/s winds normalized per station per month for all 41 PAM stations during COHMEX (Fujita, 1987).

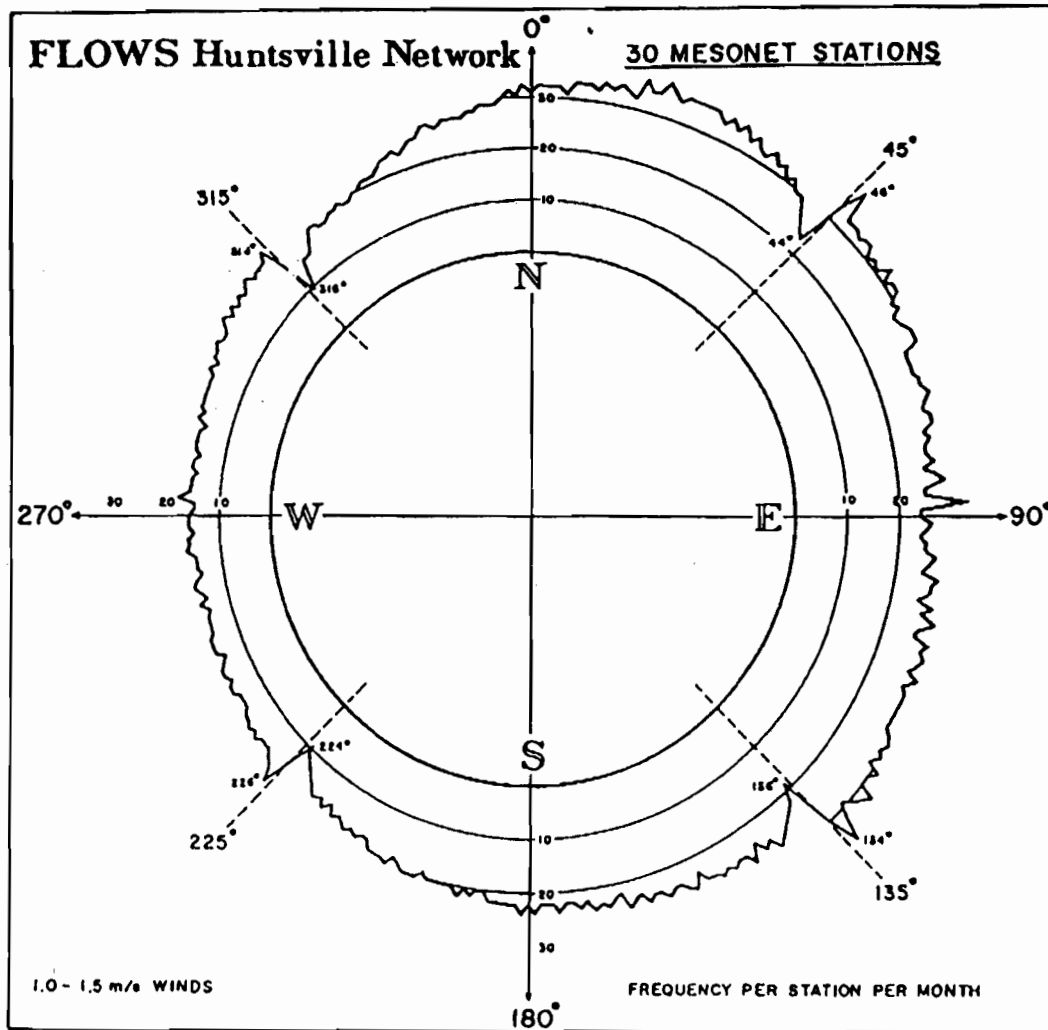


Figure 12. Azimuthal frequency of 1.0 – 1.5 m/s winds normalized per station per month for all 30 FLOWS stations during COHMEX (Fujita, 1987).

discrepancy in the frequency of measurements at the transition angles (Fig. 12) as was again noted by Fujita.

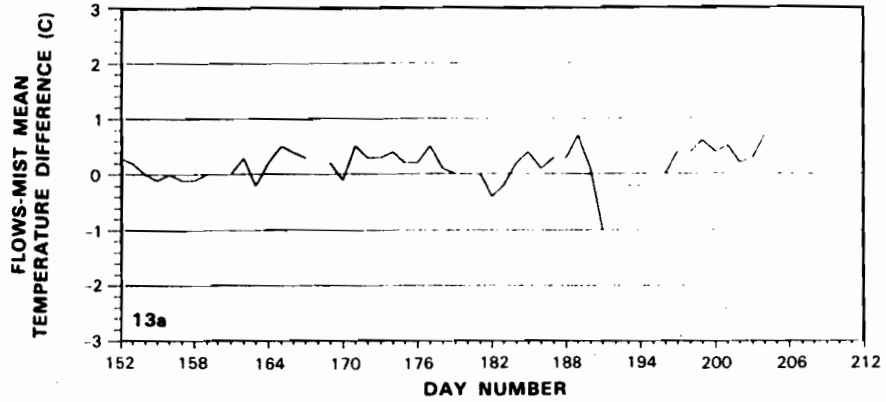
### C. Temperature and Relative Humidity

Since relative humidity is heavily dependent on temperature, the results for relative humidity and temperature were similar and they are discussed together here. During the entire period of COHMEX the difference between the daily FLOWS and MIST mean temperatures never exceeded  $\pm 1.0^{\circ}\text{C}$  (Fig. 13a), and there was a slight tendency for FLOWS to record higher temperatures. The relative humidity measurements differed by  $\pm 2\text{--}5\%$  and there was a tendency for MIST stations to record higher mean relative humidities (Fig. 14a).

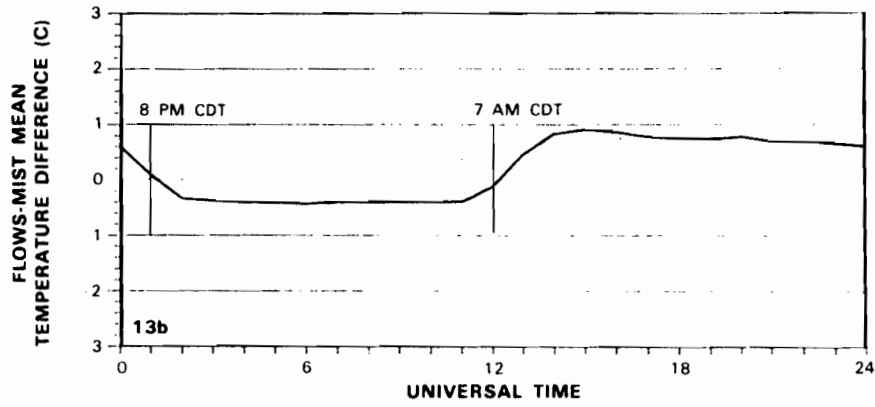
The plot of FLOWS and MIST temperature difference as a function of time of day (Fig. 13b) and the corresponding plot for relative humidity (Fig. 14b) showed a pronounced diurnal variation. During daylight hours (7 a.m. to 8 p.m.) FLOWS temperature was on the order of  $1.0^{\circ}\text{C}$  higher than MIST and FLOWS relative humidity, 5% lower than MIST. At night, FLOWS temperature was roughly  $0.4^{\circ}\text{C}$  lower, while FLOWS humidity was about 1% higher. That Figs. 13b and 14b are nearly mirror-images makes sense in that relative humidity changes vary inversely with temperature changes when there is little change in the moisture content of the air. Since that was the case on most days, it was valid for the two month average as well.

Figure 15 demonstrates that the diurnal variation described above was due to differences in wind speed. These two plots are similar to Fig. 13b, but they each represent only single days: one with high winds (Fig. 15a, 4 June 1986), and the other with low winds (Fig. 15b, 1 June 1986). On the high wind day there was almost no variation and the two networks recorded very nearly the same values. On the low wind day, the diurnal change was large and there was more than a  $2^{\circ}\text{C}$  difference in measured temperature. Figure 13b is thus an average of the plots for many days with curves that vary between Figs. 15a and 15b.

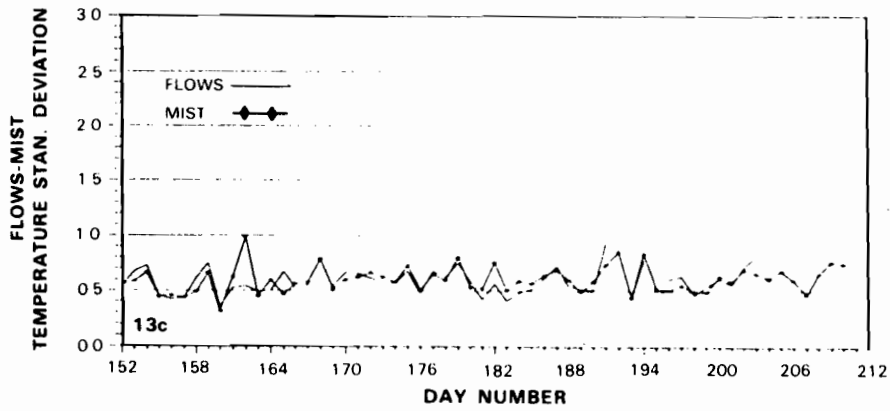
Inadequate ventilation of the FLOWS temperature and relative humidity probe was the most likely cause of the error in the measurement of temperature and relative humidity. In light winds the vane aspirator may not have remained turned into the wind and the airflow may simply have been too weak to prevent the air's warming inside the vane. The MIST stations would not display such an error since their dry and wet bulbs were kept fan-ventilated at a rate of 4 m/s. Figure 16 also demonstrates that the largest temperature difference between the networks occurred at the lowest wind speeds. It was unlikely, though, that such an error would diminish the ability of the FLOWS network to operate effectively during the windy conditions near thunderstorms.



A. NETWORK TEMPERATURE DIFFERENCE vs DAY NUMBER



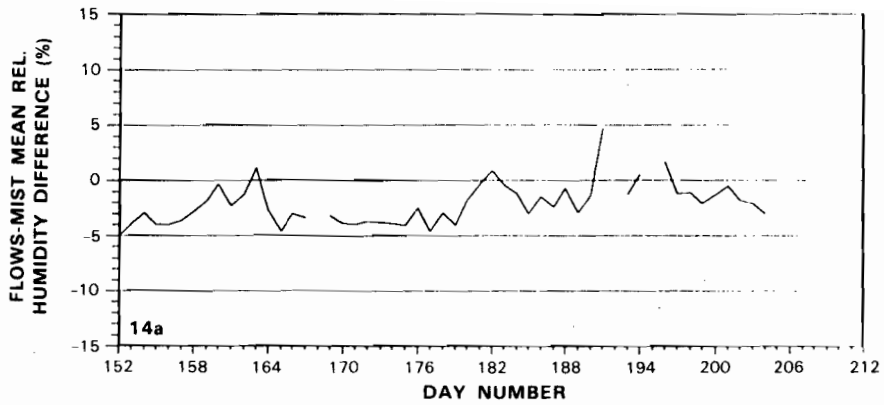
B. NETWORK TEMPERATURE DIFFERENCE vs TIME OF DAY



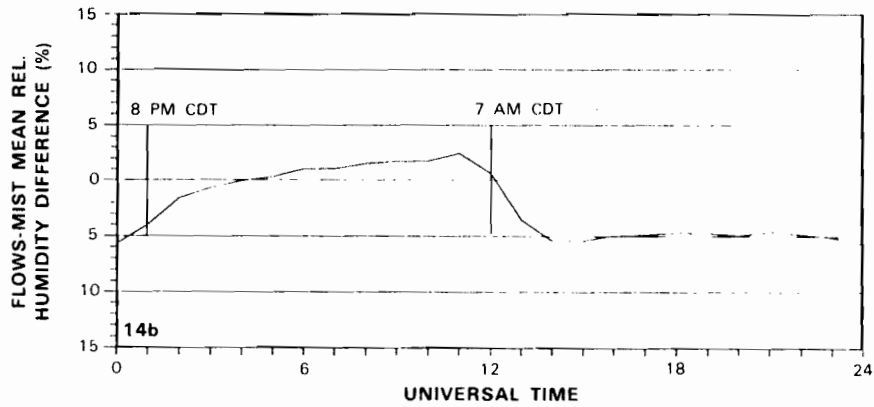
C. STANDARD DEVIATION OF TEMPERATURE FOR EACH NETWORK

Figure 13. Temperature comparison data for FLOWS and MIST networks.

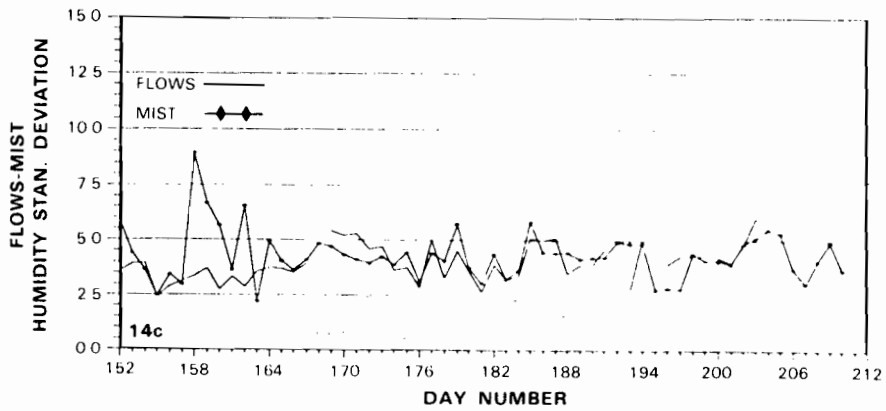




A. NETWORK RELATIVE HUMIDITY DIFFERENCE vs DAY NUMBER

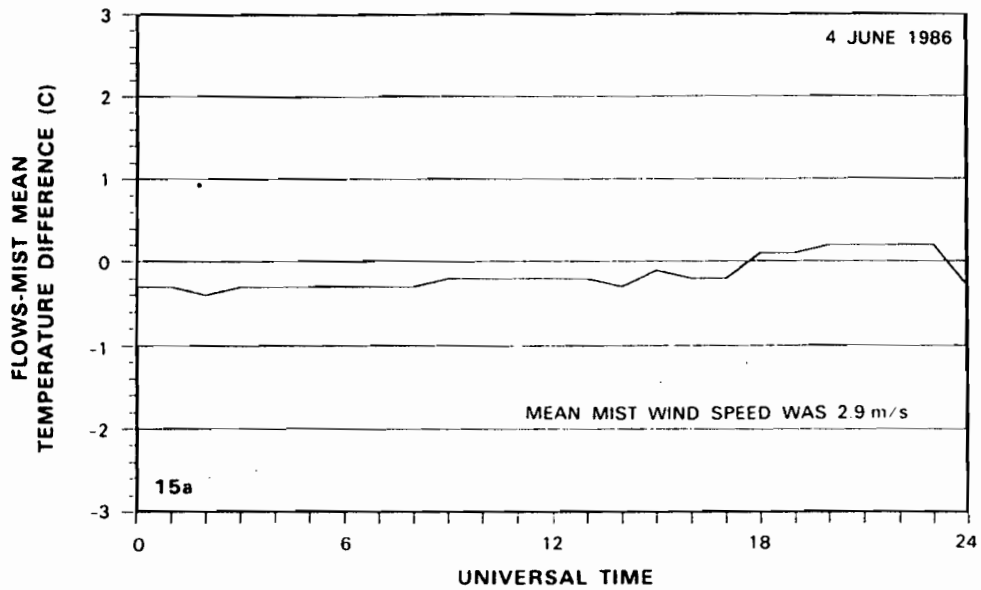


B. NETWORK RELATIVE HUMIDITY DIFFERENCE vs TIME OF DAY

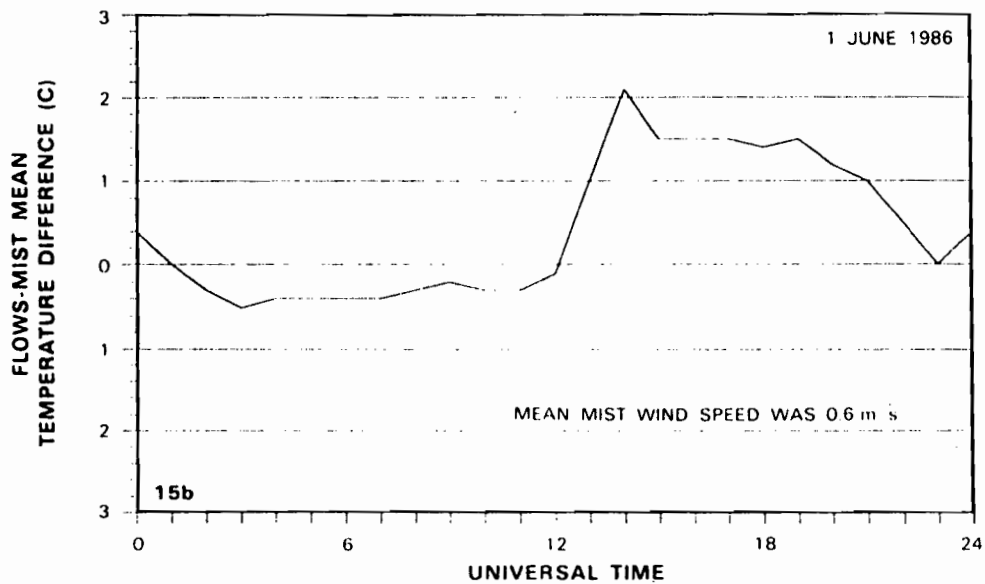


C. STANDARD DEVIATION OF RELATIVE HUMIDITY FOR EACH NETWORK

Figure 14. Relative humidity comparison data for FLOWS and MIST networks.



**A. NETWORK TEMPERATURE DIFFERENCE vs TIME OF DAY FOR HIGH WIND SPEED DAY**



**B. NETWORK TEMPERATURE DIFFERENCE vs TIME OF DAY FOR LOW WIND SPEED DAY**

Figure 15. Difference between FLOWS and MIST network average temperature vs. time of day (GMT) for a high wind speed day and a low wind speed day.

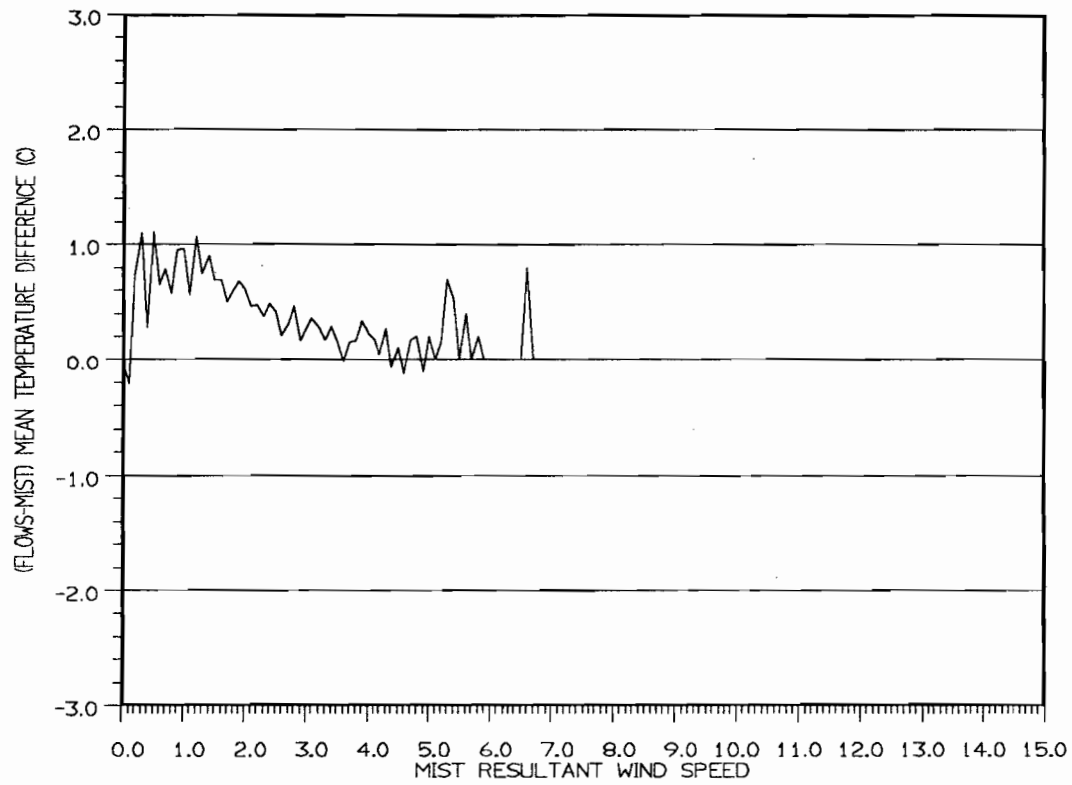


Figure 16. Network temperature difference vs. MIST average wind speed.

#### D. Barometric Pressure

The plotted results for the network pressure differences are shown in Fig. 17. During the first six weeks, FLOWS pressures were generally about 2 mb higher than MIST. That excess later dropped to 1.3 mb near the end of the experiment. The levelness of the curve in Fig. 17a is an indication of an absolute calibration error, probably in the FLOWS network. Figure 17b reveals a very slight diurnal variation. In Fig. 17b FLOWS is also roughly 2 mb higher than MIST pressure, with the largest discrepancy occurring just after the coolest part of the day at dawn, and the smallest difference occurring just after the warmest part of the day before sunset. Perhaps, this is evidence of the known temperature sensitivity of the FLOWS barometers, although the current calibration equations do take sensor temperature into account.

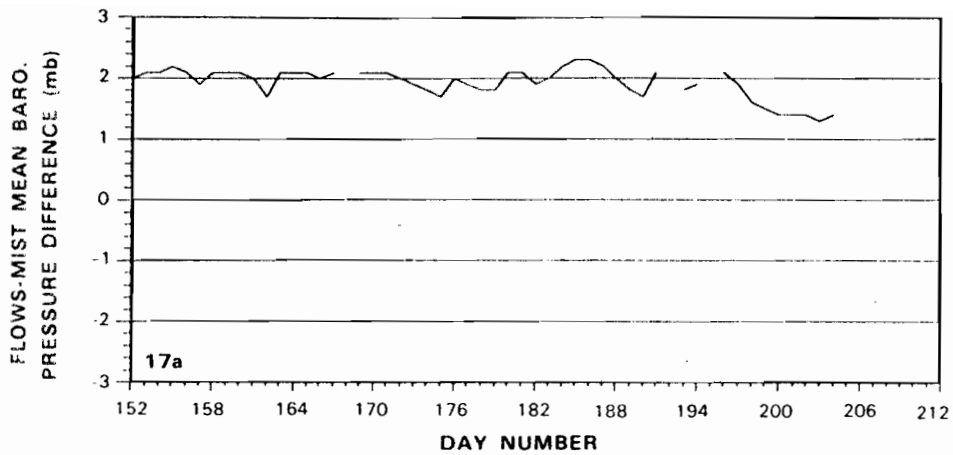
The standard deviation curves in Fig. 17c show less consistency in the FLOWS barometers than the MIST instruments. The average deviation for each network was just under 1 mb. There were several long periods in which FLOWS displayed less noisy pressure readings than MIST as well as three days on which FLOWS recorded much more noisy readings than MIST. For much of the two-month period the barometers from both networks operated with a resolution of around 1 mb.

#### E. Total Precipitation Amounts

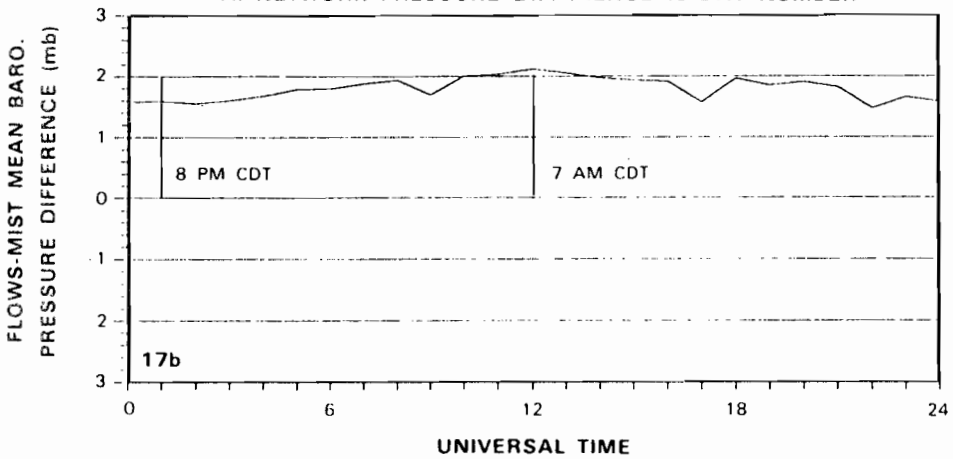
Precipitation data could not be averaged and compared across the networks in the same way as the other data because rain events were extremely localized in space and time. Nevertheless, a meaningful comparison of the relative network ability to measure total precipitation amounts could be obtained by comparing that data for pairs of FLOWS and MIST stations which were close to each other.

Eight pairs of stations were chosen for the network comparison of total precipitation amounts (see Table 1). In addition, a pair of proximate FLOWS stations (pair No. 9) and a pair of proximate MIST stations (pair No. 10) were included as "controls" to determine the differences encountered between stations with identical rain gages but slightly different location. The locations of the 10 pairs of stations are shown in Fig. 18.

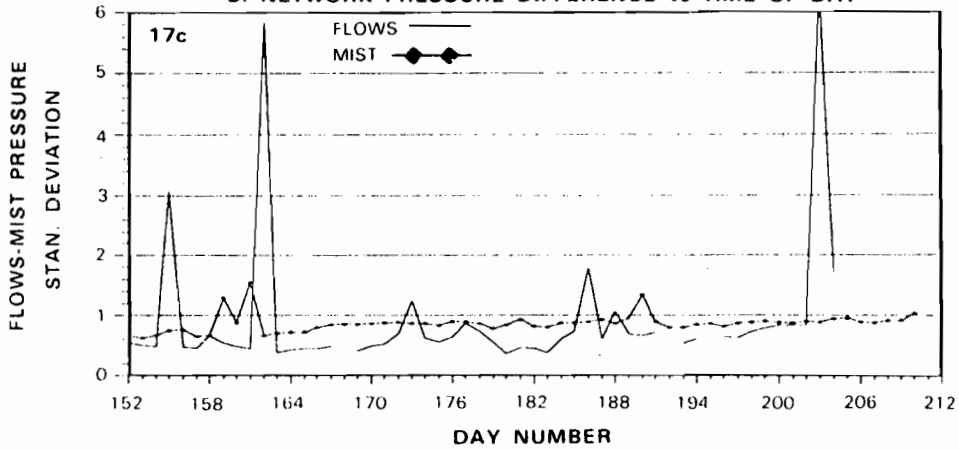
Nine precipitation events with significant rainfall amounts were chosen from the COHMEX dataset. The day number, time period, and mean total rainfall averaged over the 17 FLOWS and MIST stations included in the study are listed in Table 2. The time interval and the total rainfall amounts roughly characterize the precipitation events; more details on the complete weather situations are available in the COHMEX data summary by Williams *et al.* (1987).



A. NETWORK PRESSURE DIFFERENCE vs DAY NUMBER



B. NETWORK PRESSURE DIFFERENCE vs TIME OF DAY



C. STANDARD DEVIATION OF PRESSURE FOR EACH NETWORK

Figure 17. Pressure comparison data for FLOWS and MIST networks.

Table 1. Pairs of stations used for the comparison of total precipitation amounts between the FLOWS and MIST networks.

Pair Number	FLOWS Station Number	MIST Station Number
1	6	24
2	12	27
3	13	33
4	15	37
5	22	28
6	22	29
7	24	35
8	26	39
9	17, 18	--
10	--	28, 29

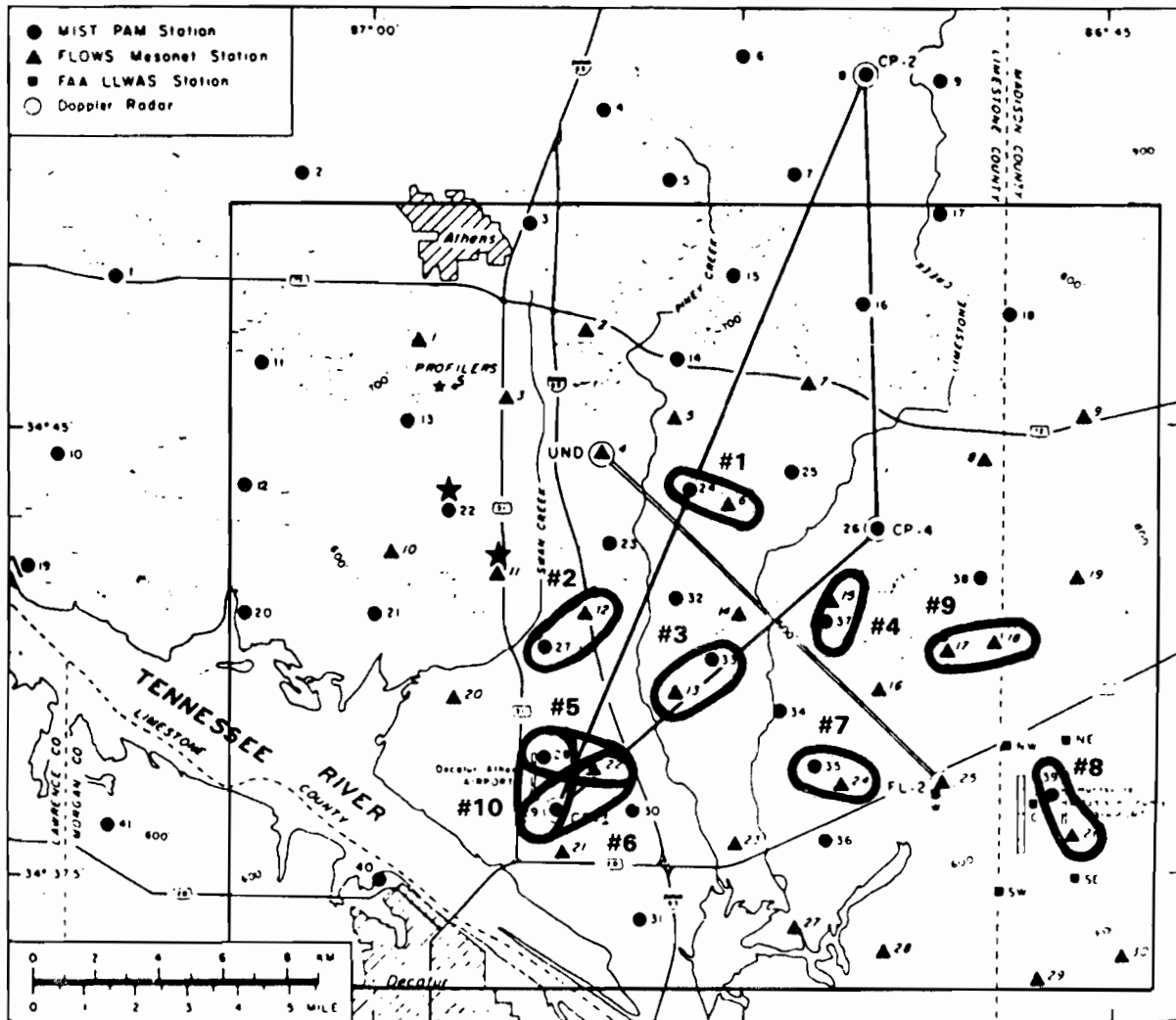


Figure 18. Location of mesonet pairs used for the comparison of network total precipitation amounts.

Table 2. Ratio of MIST total rainfall to FLOWS total rainfall for the COHMEX precipitation events listed.

DAY	TIME (GMT)	AVG TOTAL RAIN (MM)	PAIR NUMBER										AVG 1-8	AVG 1-10
			1	2	3	4	5	6	7	8	(CONTROLS)			
154	1830 - 2000	2.8	-	6.23	1.25	1.00	4.43	1.00	-	1.00	1.00	4.43	2.48	2.54
158	1630 - 1800	8.6	7.67	4.25	1.40	2.12	1.92	1.73	5.60	M	2.67	1.11	3.53	3.16
159	2200 - 2359	23.1	3.63	1.60	1.45	1.17	1.35	1.29	1.84	2.70	0.69	1.05	1.88	1.68
163	0000 - 0200	14.6	5.03	1.10	1.58	2.87	1.25	1.36	1.61	1.49	1.46	0.93	2.04	1.87
168	1930 - 2100	5.9	5.25	1.67	1.56	-	0.60	0.55	0.47	-	1.00	1.09	1.68	1.52
180	0800 - 1400	54.8	1.31	0.83	1.39	1.65	0.60*	0.60*	0.85	1.13	0.97	1.04*	1.05	1.04
183	**1630 - 1730	6.1	1.36	0.36	2.79	1.33	0.87	1.33	0.84	1.09	1.15	0.65	1.25	1.18
194	2000 - 2200	17.3	1.55	0.17	1.39	1.84	0.93	1.46	0.99	1.19	1.04	0.63	1.19	1.12
195,6	2320 - 0100	5.8	3.15	1.00	0.93	2.70	1.05	1.43	1.52	-	4.33	0.74	1.68	1.87
AVERAGE OVER ALL EVENTS:			3.62	1.91	1.53	1.84	1.44	1.19	1.72	1.43	1.59	1.30		
AVG (OMIT HIGH & LOW VALS):			3.33	1.54	1.43	1.80	1.14	1.21	1.28	1.23	1.33	0.94		

\*Data from 0800 - 1230 only were used for these pairs.

\*\*FLOWS data from 1500 - 1630 were missing.

The data listed here for pair No. 9 are the ratios of the total rainfall at FLOWS station No. 17 to that at FLOWS station No. 18; pair No. 10 data are the similar ratios of MIST No. 28 to MIST No. 29. A "-" entry indicates that the ratio was infinite, *i.e.*, that the MIST gage recorded some rainfall while the FLOWS gage recorded none; these entries were omitted from the calculated averages. The "M" entry indicates that data from one of the stations were missing. The two columns at the far right show the average of the ratios for pair Nos. 1-8 and pair Nos. 1-10. The bottom two rows show, respectively, the average ratio for each pair of stations over all events examined, and the average ratio for each pair of stations over all events excluding the event with the highest (non-infinite) ratio and the event with the lowest ratio.



The averages of the total rainfall ratios over all events for the control station pairs No. 9 (FLOWS) and No. 10 (MIST) exemplified the variability expected between proximate stations with identical rain gages; those values were  $1.59 \pm 1.11$  and  $1.30 \pm 1.12$ , respectively. When the highest and lowest total rainfall ratios were eliminated before computing the mean and standard deviation, the values became  $1.33 \pm 0.57$  for the FLOWS control pair and  $0.94 \pm 0.17$  for the MIST control pair. Judging from the values listed for other pairs (bottom two rows of Table 2), we concluded that FLOWS gages did measure, on average, lower total precipitation amounts than the MIST stations. Four of the eight pairs (Nos. 1–8) had average (omitting the highest and lowest values) ratios greater than the FLOWS control mean (1.33), but only one pair (No. 1) had a value greater than the FLOWS mean plus one standard deviation. All of the pairs had values greater than the MIST control mean (0.94) and also had values greater than the MIST control mean plus one standard deviation.

Further examination of Table 2 shows that the ratio of MIST to FLOWS total precipitation amounts was highly dependent on the type of rain event. When the average ratio for pair Nos. 1–8 for each event (second column from the right in Table 2) was greater than either of the controls (third and fourth columns from right), there was an indication that the FLOWS gages were reporting lower rainfall amounts. That was the case in roughly two thirds of the events. Day 180 was characterized by long periods of very heavy, uniformly distributed rainfall and very light winds; peak wind speed values rarely reached 5 m/s. It was the only day on which the MIST and FLOWS gages agreed, thus ruling out the possibility of an absolute calibration error. Days 154, 168, and 195 were characterized by short localized bursts of high winds and heavy rain but by less total precipitation; for several station pairs on those days the FLOWS station recorded no rain while the corresponding MIST station picked up from 0.25 to 6.25 mm (“–” entries in Table 2). That indicated a lack of sensitivity of the FLOWS gages and perhaps some influence of wind speed on the FLOWS measurement of precipitation. The anomalously high average ratio over all events for pair No. 1 suggested that local conditions may have influenced the FLOWS rain gage exposure, or that some miscalibration may have existed.

One possible explanation for the discrepancy between the FLOWS and MIST rain data was that the PAM-II rain gages were overreporting rainfall amounts. (Tipping bucket gages can sometimes become unstable and tip before they are full due to excess vibration during periods of high winds). However, it was equally likely that the PAM-II system underreported rainfall amounts, because rain that fell during the finite time it takes for the bucket to tip was never recorded by the gage. If, instead, the FLOWS gages were underreporting total rainfall amounts and the observed discrepancy was not caused by calibration errors, then we would have to find other

explanations. First, contributions to the total measured rainfall by light precipitation might have been measured inaccurately by the FLOWS gages, but that would not account for the observed discrepancy. Second, the problem may be in the measurement of rainfall during high wind conditions. The tapered neck of the gage, the 8 inch collection diameter, and the location of the gage relative to the station may have played a role. There is a known transient effect of lifting or lightening of the rain gauge bucket during high winds because of pressure forces inside the gage. This would have lead temporarily to lower rain rate measurements but should not have affected the total precipitation amount recorded for the events. (Chapter V discusses a weather event in which high winds may have influenced the FLOWS rainfall measurement).

If the underreporting of rainfall by the FLOWS gages was on the order of 5-10% (ratios of 1.05 - 1.10) there would be little cause for concern. However, the observed ratio of MIST to FLOWS total rainfall was  $1.62 \pm 0.68$  (using the averages computed after the highest and lowest ratios for each pair had been omitted) and total rainfall estimates commonly differed by a factor of 2 or more. The accurate correlation of rainfall rate to surface outflow speed is critical if correct conclusions about thunderstorm downdraft or "downburst" forcing mechanisms are to be drawn.

## V. DOWNBURST EVENT OF 7 JUNE 1986

This brief case study is intended to demonstrate how the PAM-II (MIST) and FLOWS networks compare operationally and to give one example of their ability to measure total rainfall amounts.

The weather on 7 June 1986 was cool and mostly cloudy with a mean FLOWS temperature of 22.8°C and a mean MIST temperature of 22.9°C. The average relative humidity for the day was just over 90%. The mean (corrected) pressure of 1013.6 mb, as measured by the MIST network, was the lowest during the two-month period. The mean wind direction for the day was from the south-southwest. Wind speeds were generally light to moderate throughout the day, exceeding 10 m/s only during a rainfall event between 1650 and 1750 GMT. Thunderstorms rapidly developed near the Tennessee River in the southwest portion of the network (see Fig. 1) around 1700 GMT, and moved northeastward during the following hour producing locally heavy rainfall and strong, gusty winds.

### A. Individual Station Comparison

An impression of the relative network data quality can be derived by comparing the data at two closely located stations. The 24-hour time series plots of data from FLOWS station No. 15 and MIST station No. 37 are shown in Fig. 19. A quick glance at these plots shows that the recorded data are similar and that the overall quality and resolution are comparable. FLOWS station No. 15 (Fig. 19a) missed a transmission at 1345 GMT so the data from 1315 – 1345 GMT are missing; MIST station No. 37 (Fig. 19b) missed none of its transmissions on this day. Evidence of the downburst event just after 1700 GMT was captured in the data of both stations: the event was characterized by a rise in pressure (see the circled number 1 on Figs. 19a and 19b), a drop in temperature (2), a rise in relative humidity (3), heavy rainfall (4), and high wind speeds (5) with associated abrupt changes in wind direction (6). Note the following points in comparing the time series data.

- The pressure traces were nearly identical in Figs. 19a and 19b although the absolute values differed by roughly 25 mb; however, the FLOWS pressure values were slightly more noisy than those for MIST because of the limited digital resolution of the FLOWS barometer signal.
- During the rain event, the relative humidity at FLOWS No. 15 reached 100% and stayed saturated for over an hour while the relative humidity at MIST No. 37 decreased after the heavy rain ended. The difference was attributed to the forced airflow over the MIST psychrometer. The saturated conditions could have been caused by wetting of the humidity sensor in the FLOWS station which can occur in very heavy rain.

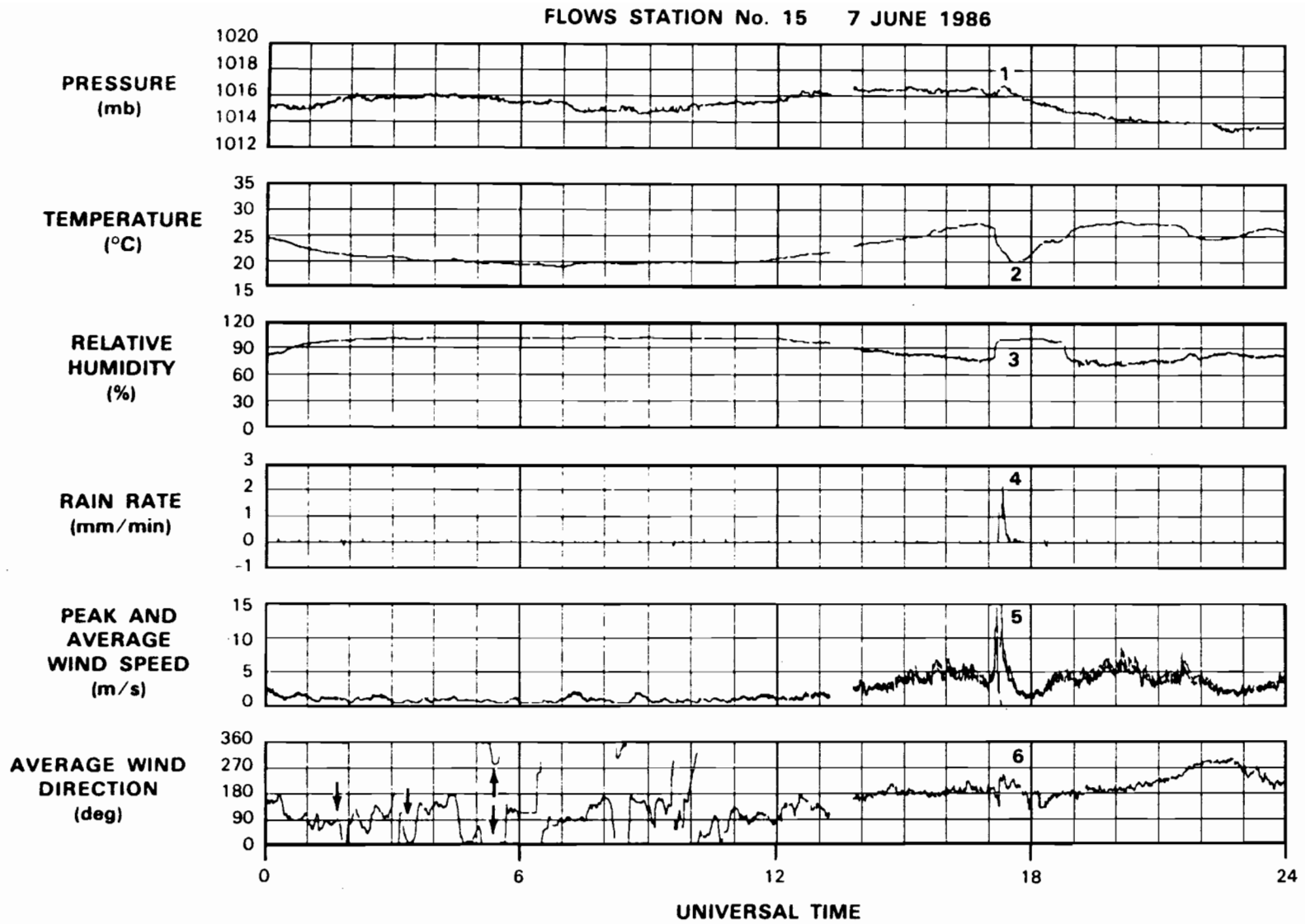


Figure 19. Comparison of 24-hour time series plots of data on 7 June 1986 (sheet 1 of 2).

MIST STATION No. 37 7 JUNE 1986

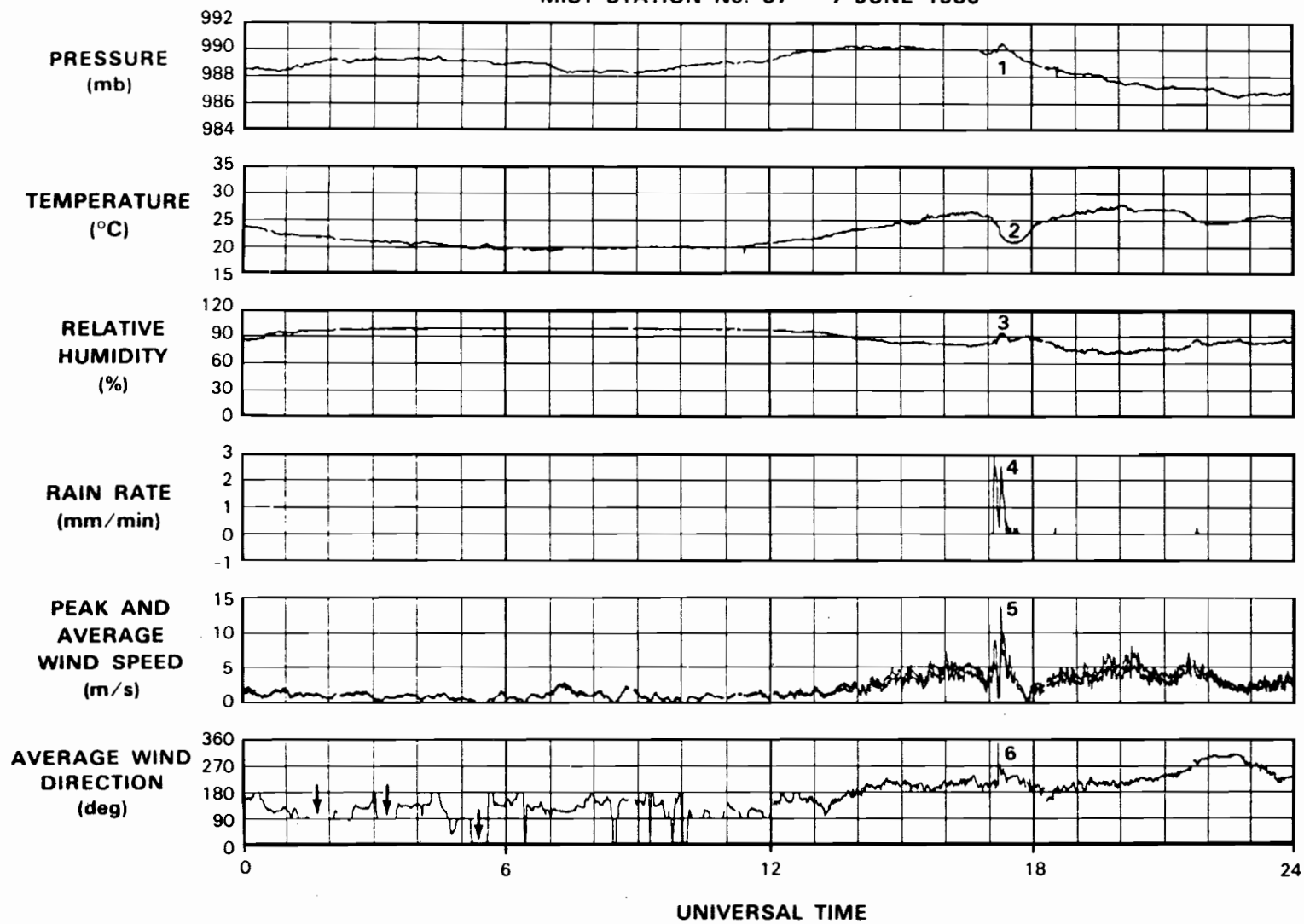


Figure 19. Comparison of 24-hour time series plots of data on 7 June 1986 (sheet 2 of 2).

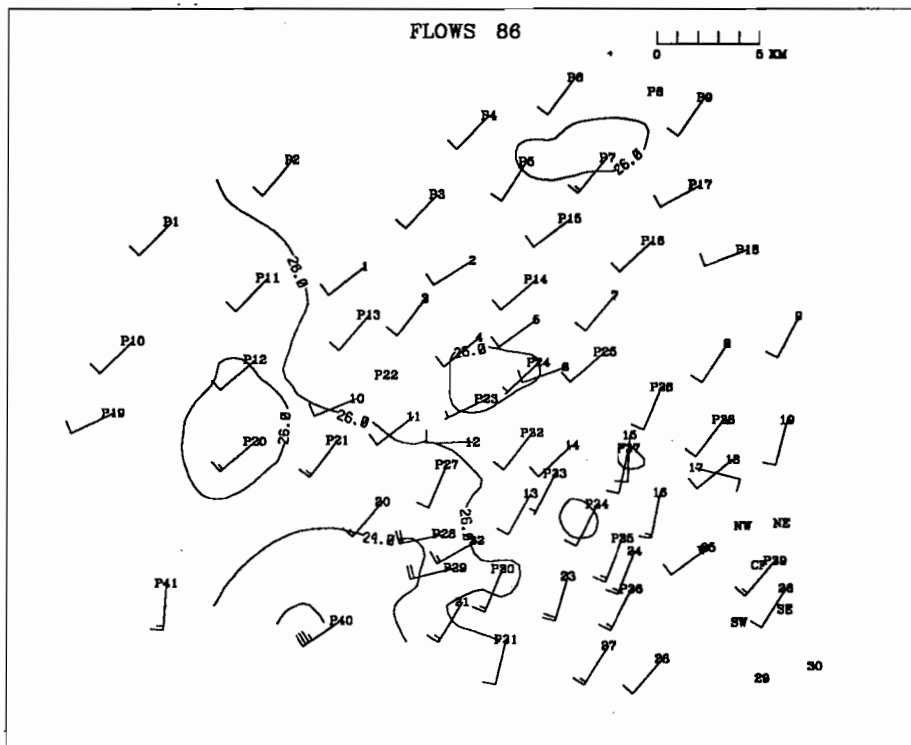
- Small artifacts showed up in the rainfall trace for FLOWS No. 15 at 30 minute intervals. They were caused by incomplete 1 minute averages resulting from the lack of availability of the processor during times of transmission to the satellite.
- The inadequacy of deriving wind direction from east and north speed components in light wind situations can be seen by comparing the wind direction traces during the first 6 hours of the day, especially from 0145–0200, 0305–0330, and 0515–0530 GMT. The wind direction at MIST No. 37 was “stuck” at 90° or at 0° while the wind direction at FLOWS No. 15 fluctuated smoothly about the azimuths.
- The temperature, wind speed (both average and peak were drawn), and wind direction traces at all but the lowest wind speeds were all highly similar.

## B. Network Comparison

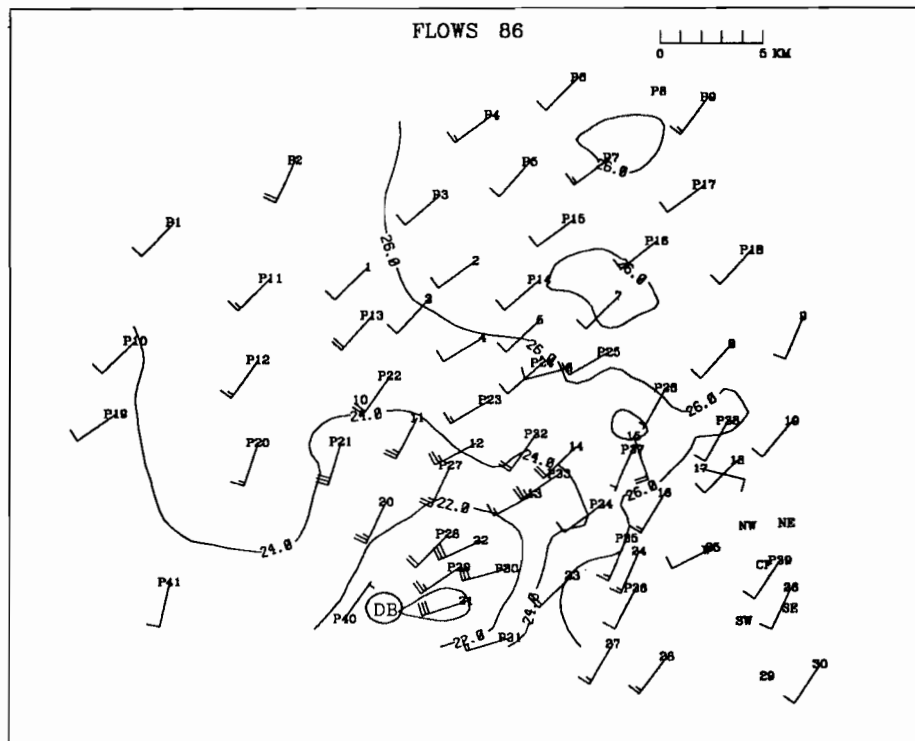
Figure 20 is a series of synoptic plots displaying FLOWS and MIST wind speed and direction, and contours of temperature at ten minute intervals from 1700 to 1730 GMT. The MIST (PAM-II) station numbers begin with the letter “P”. The winds are plotted so that the station number is at the “head” of the arrow pointing in the direction toward which the wind is blowing. The “barbs” on the tail of the arrow represent the wind speed; a long barb represents 5 m/s or roughly 10 kts and a short barb represents half of that. Temperature data from all of the stations are used to draw the contours.

At the time of the first plot (Fig. 20a) a heavy thunderstorm was approaching the area from the southwest. It proceeded northeastward directly across the networks while dropping a band of very heavy rain. The plots show the advance of the downdraft-generated cooler air, which roughly corresponds to the region of rainfall. Note the overall agreement of the wind speed and direction measurements from each network and the smooth temperature contours. In Fig. 20b, the downburst (marked “DB”) is centered near station No. P40 near the southern edge of the network. High speed winds could be seen diverging from that point towards the northeast, the direction in which the storm itself was propagating. Comparing Fig. 20b with Fig. 20c shows that the cold thunderstorm air and high wind speeds along the storm’s leading edge proceeded northeastward. By 1730 GMT (Fig. 20d) the high wind speeds had subsided as the associated temperature contrast diminished; the cool downdraft air had largely replaced the warmer air that was present before the storm arrived.

The total precipitation measured during the thunderstorm by each network separately, and by both networks combined, is shown in Fig. 21.

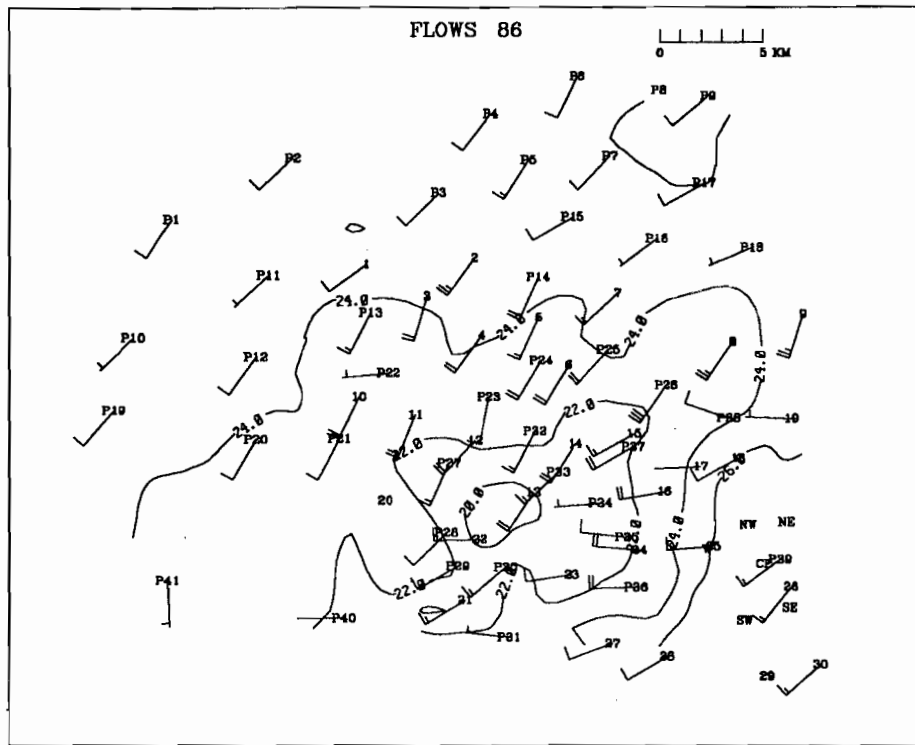


a. Map at 1700 GMT.

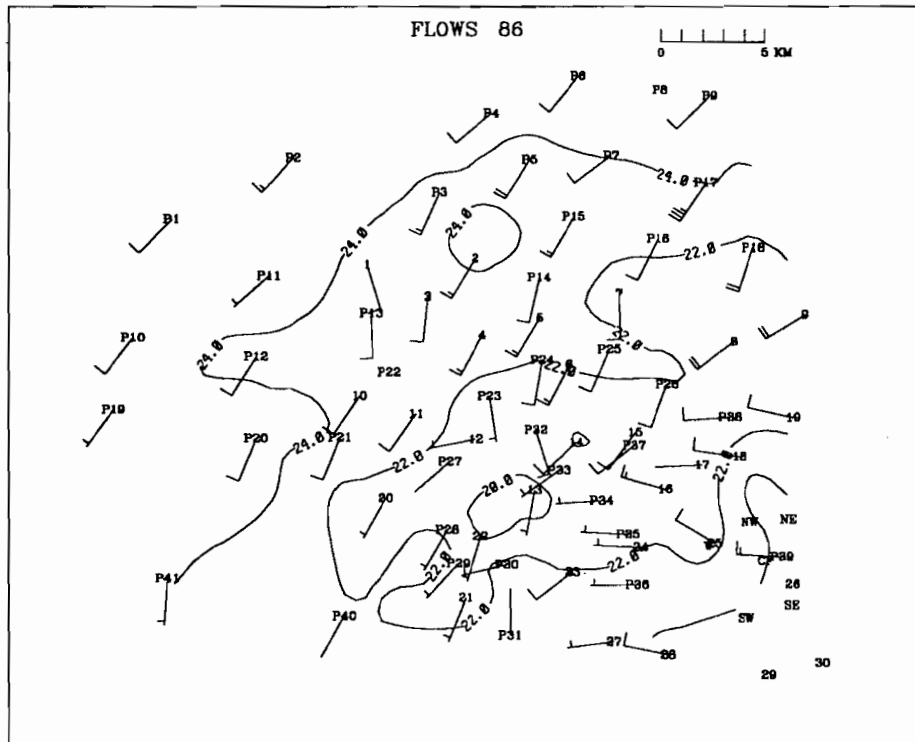


b. Map at 1710 GMT.

Figure 20. Surface wind field and temperature contours (every 2 deg. C) over FLOWS and MIST networks on 7 June 1986 (sheet 1 of 2).



c. Map at 1720 GMT.



d. Map at 1730 GMT.

Figure 20. Surface wind field and temperature contours (every 2 deg. C) over FLOWS and MIST networks on 7 June 1986 (sheet 2 of 2).



# FLAWS NETWORK

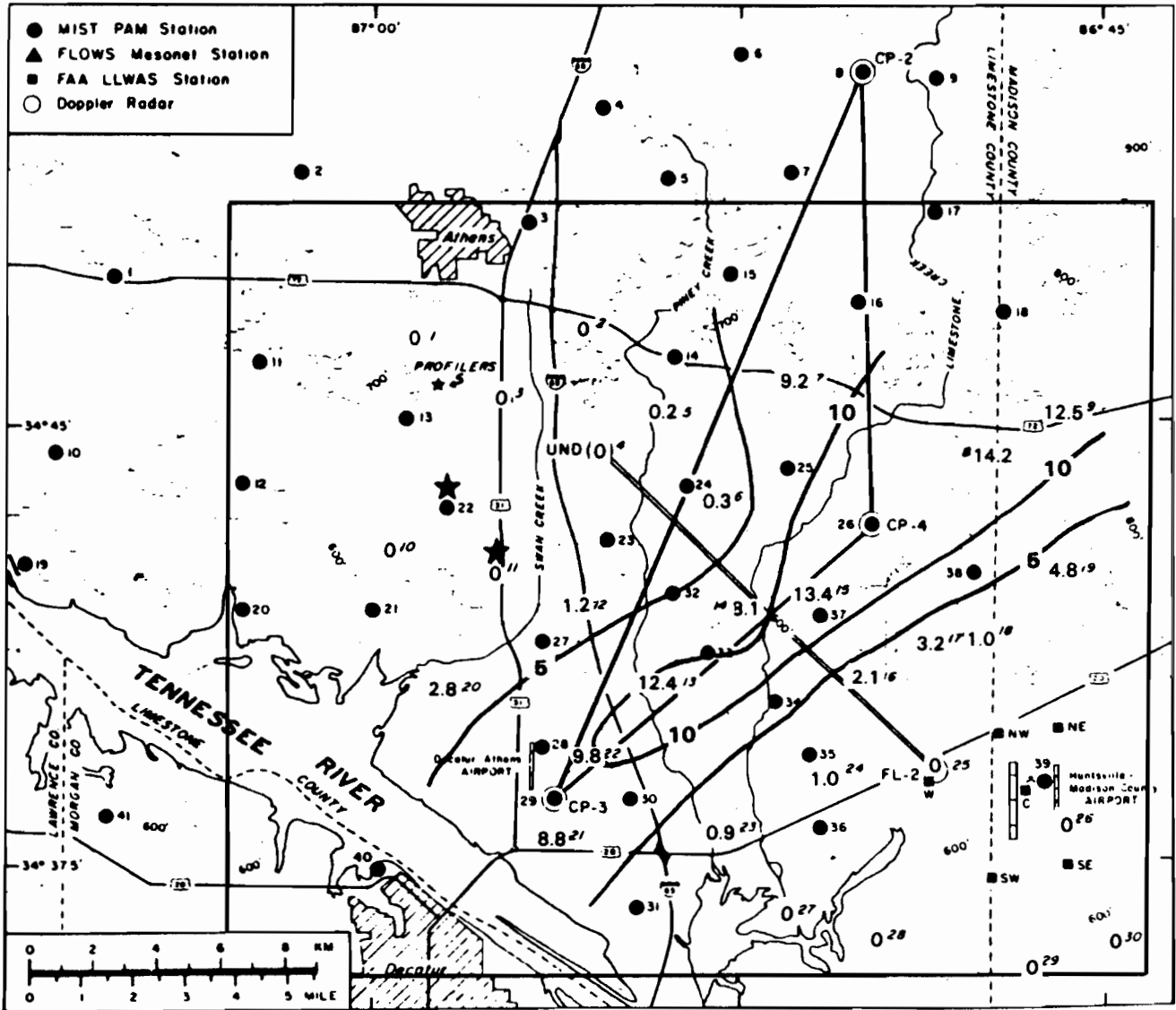


Figure 21. Total precipitation amounts (mm) for 7 June 1986, 1650-1750 GMT (sheet 1 of 3).

# MIST NETWORK

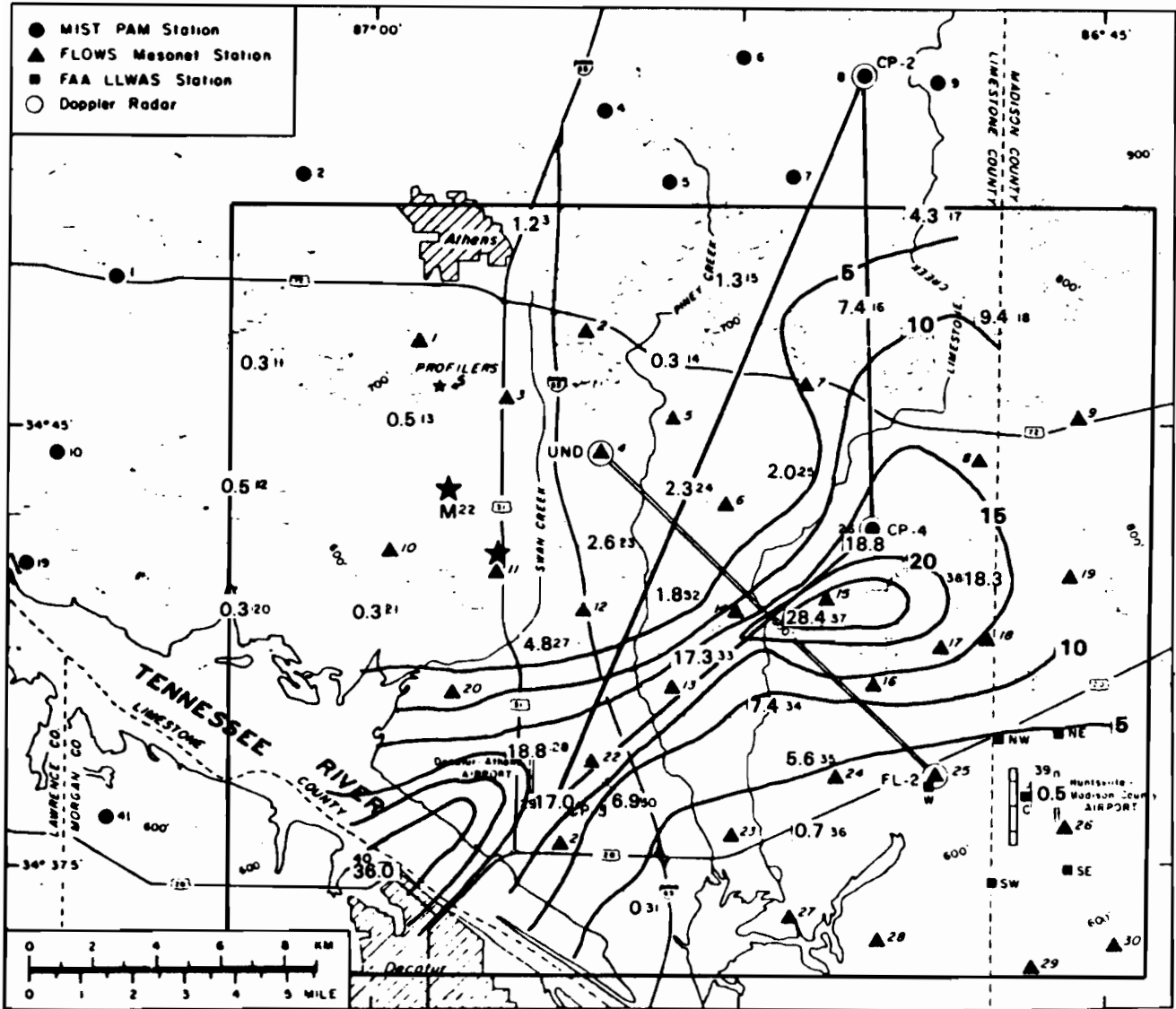


Figure 21. Total precipitation amounts (mm) for 7 June 1986, 1650-1750 GMT (sheet 2 of 3).

# MIST/FLOWS NETWORK

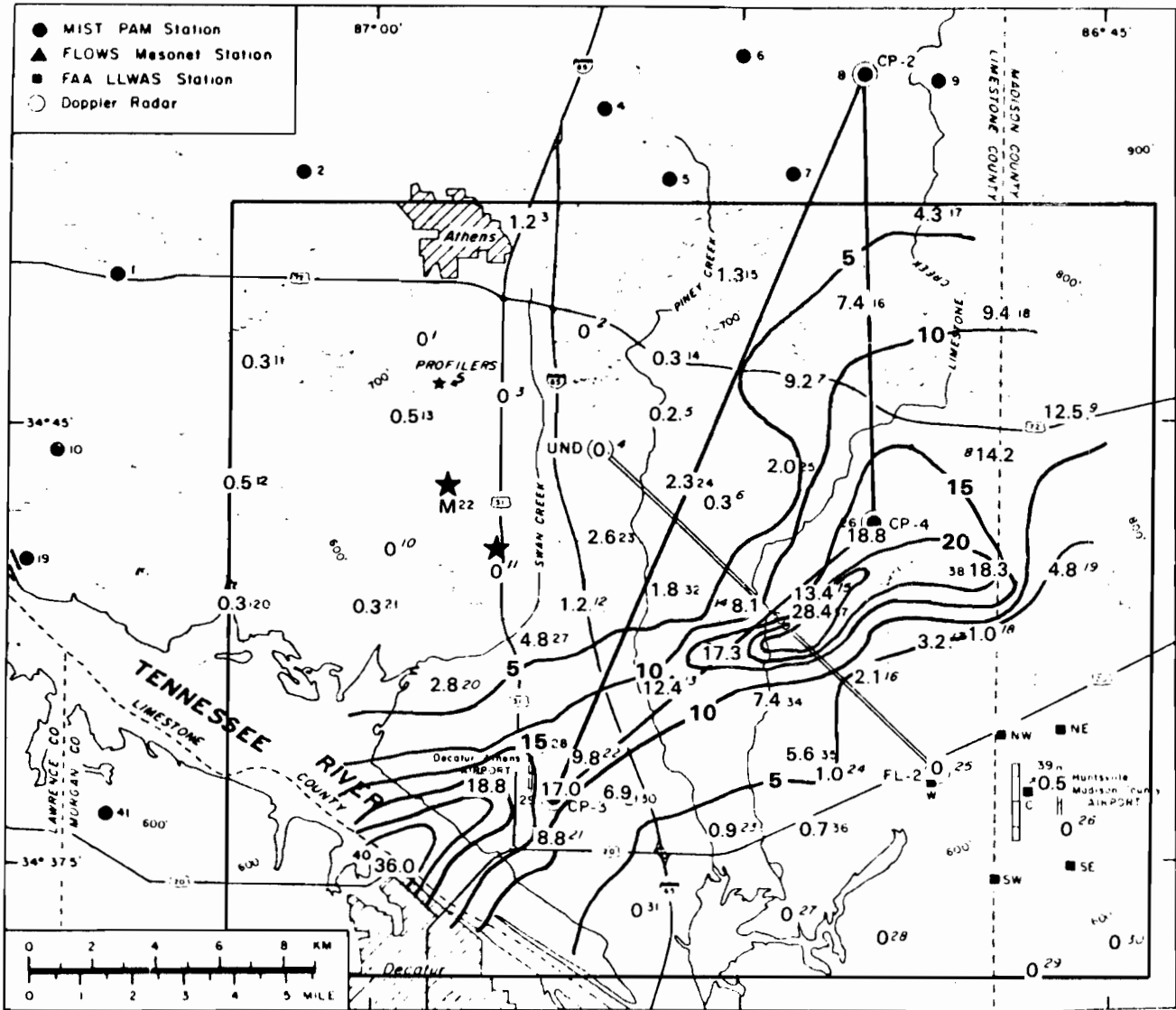
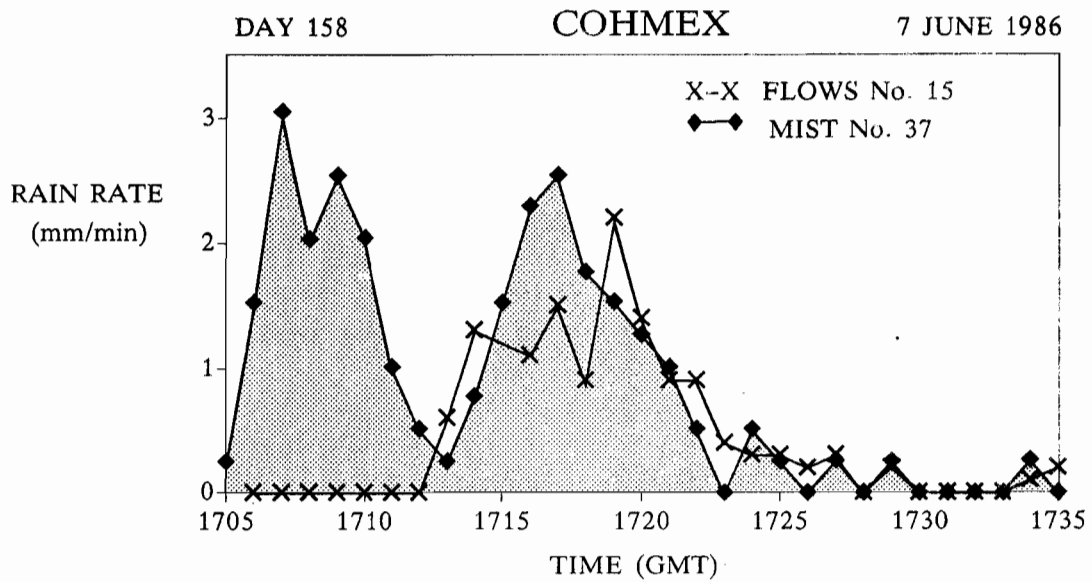


Figure 21. Total precipitation amounts (mm) for 7 June 1986, 1650-1750 GMT (sheet 3 of 3).

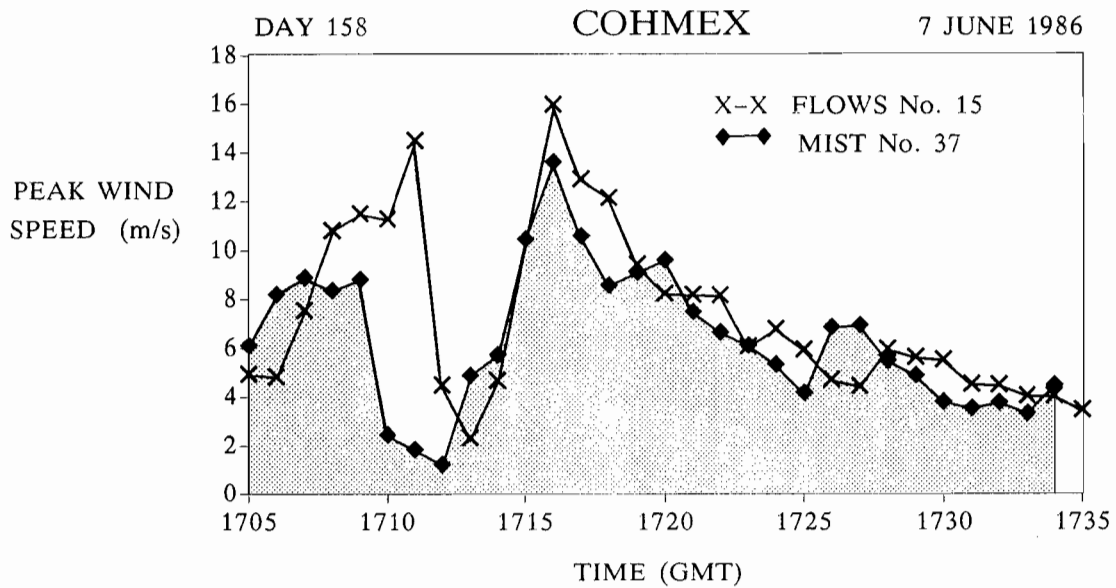
Although each network showed the band of heavy rain, the MIST (PAM-II) rain gages (Fig. 21b) collected total rainfall amounts from 1.5 to 2.0 times greater than the FLOWS rain gages (Fig. 21a). Figure 21c shows the effect of using the two networks of rain gages combined. The degree of fine scale structure revealed in the contours and the extremely tight gradients near the zone of maximum rainfall may be unrealistic. However, the rain events themselves were localized.

It is interesting to compare the rainfall rate as a function of time during the event at FLOWS station No. 15 with that at MIST No. 37 (Fig. 22a). Those stations were in the center of the zone of maximum rainfall (north of the Tennessee river) and their total rainfall amounts were 13.4 mm and 28.4 mm, respectively. (The 24-hour time series plots for the same two stations are shown in Fig. 19.) Figure 22a shows that the MIST station recorded two surges of rain while the FLOWS station recorded only one; that alone accounts for most of the large discrepancy in the total rainfall amounts. The peak wind speed traces for the same time period are shown in Fig. 22b. The curves show the FLOWS station's data lagging the MIST data by 1-2 minutes which is to be expected since MIST No. 37 is about 1 km south-southwest of FLOWS No. 15.

The FLOWS station recorded much higher peak wind speeds than did the MIST station from 1705 to 1713 GMT; during the same time only the MIST station recorded any rain. This suggests that the lack of rain at the FLOWS station for this time period may be real, *i.e.*, that the two stations were actually sampling different parts of the storm. If they were not sampling different parts of the storm, this could be a dramatic example of high winds suppressing the rainfall measurements at a FLOWS station. During the following 10 minutes high speed winds and high rain rates were recorded at both the FLOWS and MIST stations. Figure 23 shows that the rain rate at the FLOWS station did not reach 2 mm/min until the peak wind speed dropped below 10 m/s, while at the MIST station high rain rates and high peak wind speeds were recorded simultaneously. Again, this could be an artifact, but it does suggest that wind speed may play a role in the FLOWS rainfall measurements.



a. Time series of rain rate data.



b. Time series of peak wind speed data.

Figure 22. Time series of a) rain rate data and b) peak wind speed data for FLOWS Station No. 15 and MIST Station No. 37 on 7 June 1986.

DAY 158

COHMEX

7 JUNE 1986

X-X FLOWS No. 15

◆ MIST No. 37

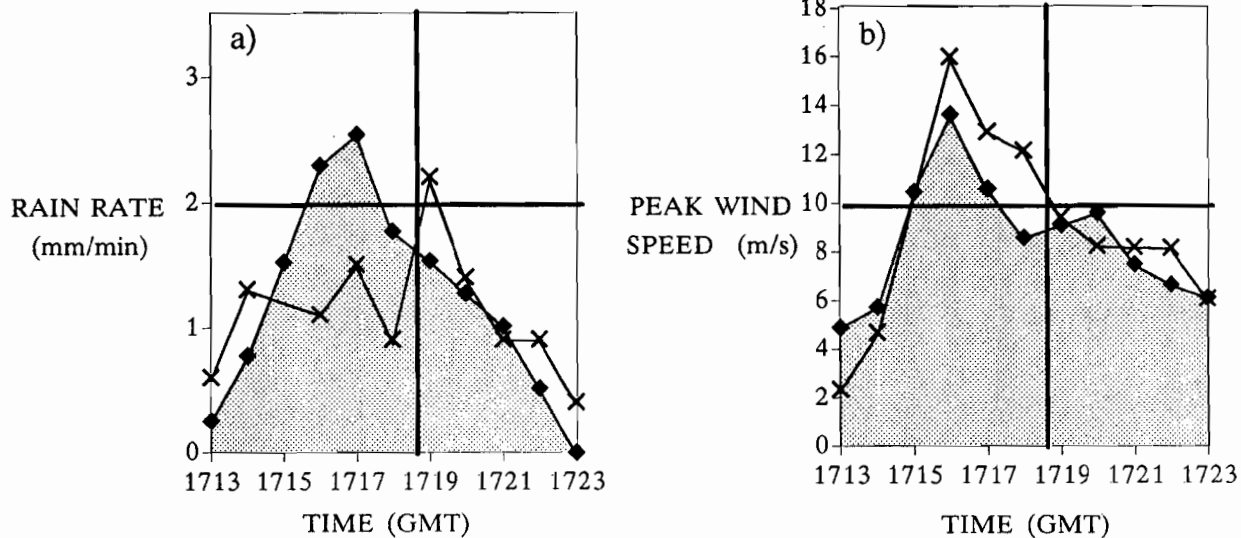


Figure 23. Time series of a) rain rate data and b) peak wind speed data during high wind speed event in which FLOWS rainfall measurements may have been suppressed.

## VI. CONCLUSIONS

For the variables most important to the detection of microbursts, wind speed and wind direction, the FLOWS and MIST networks performed with comparable accuracy during COHMEX. The FLOWS values for wind speed were consistently slightly high under all conditions, probably because of both the use of an incorrect flow coefficient and the differences in computing the 1-minute averages before the data were transmitted. The best agreement between the networks occurred in the measurement of wind direction, temperature, and humidity during moderate to high wind conditions. During low wind conditions, poor ventilation of the FLOWS temperature and relative humidity sensors became a differentiating factor as did the measurement of wind speed components (instead of wind direction directly) in the MIST stations. The periods of inaccurate pressure readings were unpredictable for both networks, but the problem of noisy pressure measurements was slightly worse for FLOWS than for MIST. The differences and discrepancies noted among these mesonet variables were all minor, and none would preclude treating FLOWS and MIST data as if they were data from one large network. We conclude that the mesonet data can be directly combined for microburst detection analyses and comparison with Doppler weather radar data (currently being pursued by J. DiStefano and D. Clark at Lincoln Laboratory).

The most serious discrepancy between the data from the two networks was found for total precipitation amounts; on average (omitting the highest and lowest ratios for each pair of stations) the PAM-II tipping bucket gages recorded 1.6 times as much rainfall as did the FLOWS weighing bucket gages. The case study presented in Chapter V revealed some of the problems encountered when using the combined networks to map total rainfall amounts. The case study also suggested a possible relationship between high wind speeds and low rainfall measurements at one FLOWS station.

## VII. RECOMMENDATIONS

To understand downburst forcing mechanisms, meteorologists need accurate correlation data for precipitation rates and surface outflow speeds. We therefore recommend further investigations of rainfall measurement data reported by the FLOWS and MIST networks for COHMEX. Particularly, the one-minute rainfall rates should be examined for all COHMEX rainfall events with special emphasis on FLOWS:MIST comparisons. If such an examination suggests that FLOWS gages underreport rainfall amounts during high wind speed events, then consideration should be given to fitting FLOWS stations with tipping bucket gages.

Additional studies should also include more rigorous determination of network agreement on different days with similar weather conditions, *e.g.*, exceedingly hot days, or very humid days, *etc.* We should also examine more closely the performances of individual stations in general as well as their performance during the extreme weather conditions that the MIST and FLOWS networks were designed to detect.



## REFERENCES

- Brock, F.V., G.H. Saum, and S.R. Semmer, 1986: Portable automated mesonet II. *J. Atmos. Oceanic Technol.*, **3**, 573-582.
- Brock, F.V., and P.K. Govind, 1977: Portable Automated Mesonet in Operation. *J. Appl. Meteor.*, **16**, 199-310.
- DiStefano, J.T., 1987: Study of microburst detection performance during 1985 in Memphis, TN. *Project Report ATC-142*, MIT Lincoln Laboratory, FAA report No. *DOT/FAA/PM-87-18*, 40 pp.
- Evans, J.E., and D. Johnson, 1984: The FAA transportable Doppler weather radar. *Preprints, 22nd Conference on Radar Meteorology*. Zurich, Amer. Meteor. Soc., 246-250.
- Fujita, T.T., 1987: Unpublished study on wind direction frequencies for FLOWS and MIST weather station networks during COHMEX.
- Williams, S.F., H.M. Goodman, K.R. Knupp, and J.E. Arnold, 1987: Space/COHMEX Data Inventory Document. *NASA Tech. Memo. 4006*, 480 pp.
- Wolfson, M.M., 1987: The FLOWS automatic weather station network. *Preprints, Sixth Symposium on Meteorological Observations and Instrumentation*, New Orleans, Amer. Meteor. Soc., 294-299.
- Wolfson, M.M., J.T. DiStefano, and B.E. Forman, 1987: The FLOWS automatic weather station network in operation. *Project Report ATC-134*, MIT Lincoln Laboratory, FAA Report No. *DOT/FAA/PM-85-27*, 266 pp.